Sustainable Materials and Technologies 45 (2025) e01435

Contents lists available at ScienceDirect

Sustainable Materials and Technologies

journal homepage: www.elsevier.com/locate/susmat

Recycling of solid oxide electrolyzer stacks

Carlo Kaiser [a,*], Sohyun Ahn [b], Martin Brünner [a], Dominik Goes [c], Jeraldine Lastam [d], Shine-Od Mongoljiibuu [a], Stephan Sarner [e,f], Alexander Specht [g], Jürgen Fleischer [c], Norbert H. Menzler [e,f], Michael Müller [d], Martin Rudolph [b], Bernd Friedrich [g], Olivier Guillon [e], Ruth Schwaiger [d], Urs A. Peuker [a]

[a] Institute for Mechanical Process Engineering and Mineral Processing, Technical University Bergakademie Freiberg, Agricolastraße 1, Freiberg 09599, Germany
[b] Helmholtz-Zentrum Dresden-Rossendorf, Helmholtz Institute Freiberg for Resource Technology, Chemnitzer Straße 40, Freiberg 09599, Germany
[c] WBK Institute of Production Science, KIT Karlsruhe Institute of Technology, Kaiserstraße 12, Karlsruhe 76131, Germany
[d] Institute of Energy Materials and Devices, Microstructure and Properties of Materials (IMD-1), Forschungszentrum Jülich GmbH, Jülich 52425, Germany
[e] Institute of Energy Materials and Devices, Materials Synthesis and Processing (IMD-2), Forschungszentrum Jülich GmbH, Jülich 52425, Germany
[f] RWTH Aachen University, Institute of Mineral Engineering, Forckenbeckstr. 33, Aachen 52074, Germany
[g] Institute and Chair for Process Metallurgy and Metal Recycling, RWTH Aachen University, Intzestraße 3, Aachen 52056, Germany

ARTICLE INFO

Keywords:
Solid oxide electrolyzer
Solid oxide cell
Recycling
End of life
Circular economy

ABSTRACT

In recent years, hydrogen has become an increasingly important energy carrier, replacing fossil fuels. In this context, electrolyzers have become a focal point of global research, as they facilitate the production of green hydrogen. Among electrolyzers, solid oxide electrolyzers are one of the most widely researched due to their high efficiency and their variability in terms of fuels and operation as fuel cells. However, due to the use of critical materials in combined with a relatively short operational lifespan, the development of recycling strategies is becoming increasingly crucial if these electrolyzers are to become a sustainable option for green hydrogen production. This study proposes the first comprehensive recycling scheme for solid oxide electrolyzer stacks. Data on the materials used by electrolyzer manufacturers from around the world was compiled and compared. Based on these materials, published recycling approaches from dismantling, mechanical recycling and metallurgy were combined with additional studies to develop a holistic recycling process aimed at recovering critical raw materials. Options for closed-loop and open-loop reuse were considered and existing gaps and challenges were identified. The current status of recycling solid oxide electrolyzer stacks demonstrates that the principle is feasible and that a significant proportion of the materials used can already be separated and recovered. However, existing gaps, such as the separation of the nickel mesh from interconnects and the separation of various oxygen ion conductors, currently result in materials being downcycled or recycled in an open loop.

1. Introduction

The harmful impact of fossil fuels on the world's climate is leading to increased interest in carbon-neutral energy technologies [1,2]. Much of this interest has been focused on renewable energy. However, renewable energy sources are subject to natural intermittency, making energy storage all the more important [3,4]. In recent years, hydrogen has become an increasingly important energy carrier and chemical reaction partner to replace carbon because it can be stored, transported and produced directly from green electricity and water [5,6]. In this context, water electrolyzers have also been of interest as they can produce green hydrogen. Based on announced projects worldwide, water electrolyzer capacities could increase from 700 MW in 2022 to 175–420 GW in 2030 [7]. As the demand for hydrogen grows, so will the demand for suitable electrolyzer technologies and the materials required for their manufacture. The three water electrolyzer technologies that are considered the most mature based on their Technology Readiness Level (TRL) are alkaline, proton exchange membrane and solid oxide electrolyzers (SOELs) [7,8]. Of these, SOELs have the highest efficiency and are characterized by the possibility of reversible operation as a fuel cell [9,10]. As this technology operates at elevated temperatures, it is ideal to for integration into chemical and/or metal, ceramic, glass and cement production using excess process heat streams. SOELs have only recently reached TRL 8 and are therefore at the beginning of the full

* Corresponding author.
E-mail address: carlo.kaiser@mvtat.tu-freiberg.de (C. Kaiser).

https://doi.org/10.1016/j.susmat.2025.e01435
Received 23 January 2025; Received in revised form 4 April 2025; Accepted 5 May 2025
Available online 6 May 2025

commercialization [7]. However, as their numbers are expected to increase, it is crucial to address an appropriate end-of-life (EoL) concept.

Recycling processes for SOEL stacks or the very similar solid oxide fuel cells (SOFCs) have not yet been introduced. However, initial strategies have been published so far, such as the EoL strategy for SOFCs as part of the HYTECHCYCLING project [11]. In their report, the authors present a process diagram for a possible EoL strategy. First, a non-destructive disassembly is performed, from which the stack components are manually sorted and separated into waste streams: the ceramic parts, the metallic parts, and the hazardous components. As with the metallic components, the ceramic components are subjected to a shredding process followed by separation. The study remains at the feasibility level as no specific technologies for separation processes have been specified. Additionally, the authors suggested existing processes for recycling yttria-stabilized zirconia YSZ and Ni/NiO by hydrothermal treatment and hydrometallurgy, respectively. A more detailed recycling concept has been published by Sarner, et al. [12] which focuses more on the solid oxide cells (SOCs). Their strategy starts with a disassembly of the stack components. Metal plates, frames, interconnects, nickel meshes and the cells have to be completely separated from each other. The metal components are treated in metallurgical processes to recover, in particular, the high-alloy steel. To ensure the required quality, they must first be separated into different grades. For the ceramic cells, the recycling strategy varies depending on the cell design. Regardless of the variations, the first step in all cell designs is the separation of the air-side electrode and contact layers. For electrolyte supported cells (ESCs), this is followed by the separation of the fuel-side electrode, with the remaining electrolyte being recycled into new electrolyte material. Fuel-side electrode supported cells (FESCs) skip the separation of the fuel-side electrode and are directly recycled with the support into new substrate material. Finally, there are the metallic supported cells that are processed pyrometallurgically. Raw materials are recovered from the separated materials for all cell designs using hydrometallurgy. Férriz, et al. [13] and Valente, et al. [14] pointed out the possibility of potential leaching for Ni recovery and the recycling of YSZ used in the cells by hydrothermal treatment according to the process of Kamiya, et al. [15]. Benedetto Mas, et al. [16] specifically reviewed the literature specifically on the leaching of La and Co from electronic waste as a possible starting point for SOC recycling.

In addition to the above recycling strategies, initial recycling approaches for individual recycling steps and components have already been published. Al Assadi, et al. [17] looked at an SOFC stack and developed a disassembly process that highlights the challenges they faced. In their approach, the stack is first compressed to remove the tensioning system. The external compression is then released and the end plate is removed from the stack. Next, the stack is disassembled. Finally, the cell frame and cell are separated, as well as the nickel mesh and interconnect.

Most recycling approaches can be found in the literature for the SOC. This is a layered structure with micron scale layers with a high concentration of critical raw materials. Saffirio, et al. [18] published a complete recycling process for the cell to recover the YSZ. In the first step, they separated the air-side layers of the cell by mechanical scraping, followed by a polishing step to remove remnants of the air-side layers and to remove the reaction barrier consisting of gadolinia-doped ceria (GDC). The remaining cell was then crushed and the YSZ structure disaggregated by hydrothermal treatment. Finally, the remaining nickel was leached with nitric acid to recover pure YSZ. A similar approach has been proposed by Yenesew, et al. [19]. In their process, the air-side layers are also separated by mechanical scraping, followed by washing with nitric acid to remove residual air-side materials. The remaining cell is then crushed and milled and the nickel is leached. Finally, the YSZ is separated from the nickel solution by sedimentation and the nickel oxide is recovered by drying the solution. Another approach specifically for FESCs was developed by Sarner, et al. [20]. The air-side layers were separated by leaching. The remaining layers, consisting of YSZ, NiO and small amounts of GDC, were milled and used as recyclate in the substrate of new FESCs. An alternative approach to separate the air-side layers was presented by Kaiser, et al. [21]. They showed that by subjecting the cell to ultrasound and cavitation, it is possible to selectively detach the air-side layers and obtain a highly concentrated perovskite material containing critical raw materials such as La, Sr and Co. Recently, Yenesew, et al. [22] published a slightly different approach to SOC recycling. They crushed and milled the cell before performing a leaching step to dissolve the perovskites and NiO. The solid YSZ is separated from the solution by centrifugation. The Ni in the solution is selectively precipitated by the addition of a precipitant and separated by subsequent filtration. To recover the perovskites, the remaining perovskite solution is dried and calcined.

This study presents the first process scheme covering the complete recycling of SOEL stacks. The focus is on planar FESC systems, which are currently the most widely used alongside planar ESCs. Due to many similarities in their structures, a number of processes can also be transferred to ESC systems. The study compiles the most commonly used materials in SOELs according to manufacturers' specifications and literature data. Based on these material compositions, the basic architecture of SOELs and the recycling approaches proposed in the scientific literature as well as our own experimental investigations, a holistic recycling chain is outlined, analyzing the individual processing steps. The first section focuses on the dismantling of SOEL stacks into their individual components using automated disassembly or mechanical recycling. Two primary material streams are generated during dismantling: metallic components and ceramic cells. The following sections systematically examine the processing of these material streams, incorporating mechanical recycling and metallurgical recovery methods, and highlight promising processes. In addition, a possible reuse of the materials (closed loop) and a potential reuse of the materials outside the electrolyzer manufacturing (open loop) will be addressed.

2. Materials

SOELs and SOFCs have comparable components and materials. Therefore, the following part refers to SOC stacks collectively and includes both in the materials overview. The most commercially available SOC stack is designed as a planar stack based on flat cells. An example of a planar stack is shown in Fig. 1. In this figure, the stack consists of two end plates, the top end plate (TP) and the base end plate (BP), with repeating units (RUs) in between.

In the following chapters, the materials of the components are derived from manufacturers and literature references. This information will be used later to derive and quantify the recycling process.

2.1. Repeating unit

RUs consist of at least two basic functional components: The interconnects and the electrochemically active cell [23]. Interconnects provide the electrical connection between RUs and the spatial separation of gases during chemical conversion in the cell [24,25]. Two types of interconnects have been developed: ceramic and metallic [24,26]. Ceramic interconnects are oxides that are very stable in oxidizing atmospheres, but their cost is high and they exhibit lower electrical conductivity at operating temperatures compared to metallic interconnects [26]. Metallic interconnects are used at lower operating temperatures and exhibit high electrical conductivity, but are not completely stable in oxidizing atmospheres [25–27]. Today, mainly metallic interconnects are used [28,29].

Table 1 shows manufacturers of SOC stacks, their specifications and the materials used. The interconnect materials can be divided into two groups: The high chromium ferritic steels such as Crofer22APU, Crofer22H, ITM and ZMG232G10, and the low-cost ferritic stainless steels such as AISI441 and SUS 430. The high chromium ferritic steels appear to be predominantly used, with Crofer22APU being particularly

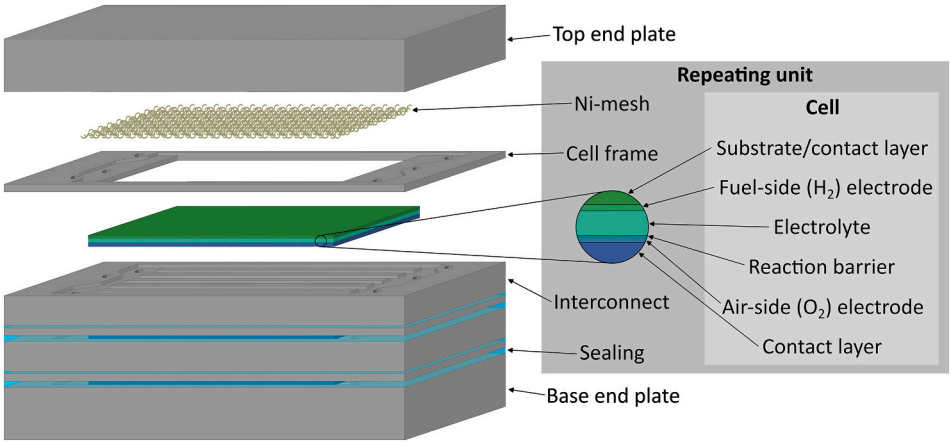

Fig. 1. Basic components of planar SOC stacks and common structure of repeating units and solid oxide cells.

Table 1
Manufacturers of planar FESC and ESC SOC stacks and related materials used in their parts and components based on literature data and company websites.

Manufacturer	Country	Operation mode	Interconnect	Cell design	Air-side materials	Electrolyte-barrier layer	Fuel-side materials	Reference
CEA/Liten	FRA	EC&FC	AISI441	FESC	LSCF LSC LSCF/GDC	YSZ-GDC	Ni/YSZ	[43,44]
Elcogen	EST	EC&FC	Ferritic metal	FESC	LSC	YSZ-GDC	Ni/YSZ	[45,46]
Fiaxell	CHE	EC&FC	Crofer	FESC	LSC LSC/GDC LSCF/GDC LSCF	YSZ-GDC	Ni/YSZ	[47]
Forschungs-zentrum Jülich	DEU	EC&FC	Crofer22APU Crofer22H ITM	FESC	LSC LSCF LCC10 LCC12	YSZ-GDC	Ni/YSZ	[48–50]
FuelCell energy	USA	EC&FC	Sanergy alloy	FESC	Perovskites	YSZ-GDC	Ni/YSZ	[51,52]
Nexceris & fuel cell materials	USA	EC&FC	ZMG232G10	ESC	LSM LSCF LSCF/GDC LSM/GDC	Sc based stabilized Zirconia	Ni/GDC Ni/SDC Ni/YSZ	[53]
				FESC	LSC	YSZ-GDC	Ni/YSZ	
SOFCMAN	CHN	FC	SUS430	ESC	LSCF/GDC	ScSZ-GDC	Ni/YSZ	[54]
				FESC	LSCF/GDC	YSZ-GDC	Ni/YSZ	
Solydera	ITA	EC&FC	n/a	FESC	LSCF/GDC LSCF	YSZ-GDC	NI/YSZ	[55,56]
Sunfire	DEU	EC	Crofer22APU	ESC	LSCF LSCF/GDC	5YbSZ YSZ-GDC	Ni/GDC	[57,58]
Topsoe	DNK	EC&FC	Crofer22APU	FESC	LSCF/GDC	YSZ-GDC	Ni/YSZ	[59–61]

common. This is consistent with the scientific literature [28,30].

Furthermore, a coating is applied to the surface of interconnects in SOC stacks to inhibit the oxidation and migration of the interconnects [31,32]. Cr diffusion in cells can be detrimental. Corrosion processes such as oxide scale growth due to Cr outward and O_2 inward diffusion are a serious concern [32–34]. Also, Cr diffusion towards the cell can poison the air-side electrode, reducing its electrochemical performance [33,35]. Commonly used coating materials are based on spinel oxides such as $MnCo_{1.9}Fe_{0.1}O_4$ (MCF) and manganese cobalt oxide (MCO) or perovskites such as $La_xSr_{1-x}MnO_{3-\delta}$ (LSM) [31–33].

Another component of the RUs is the cell frame, which is used to provide additional mechanical support in the stack and which offers required gas porting [34,36,37]. The cell frame is typically made of the same material as the interconnect [36].

Sealants are used in SOC stacks to prevent leakage and mixing of air from the air side and hydrogen gas from the fuel gas side during long-term operation [34,38]. Various sealant materials have been studied in SOELs and SOFCs, including metals, glasses, glass-ceramics, cements and composites [39,40]. Two sealing methods are applied in SOC stacks: Compressive sealing and rigid sealing [41,42]. Of the materials studied, glass and glass-ceramics appear to be the most suitable for rigid seals, as they best meet the numerous requirements [38,41]. Within these groups, borosilicates are the most commonly used, although there are still significant differences in the elements and materials added [12,38]. For compressive seals, mica-based and glass-ceramic materials are the most widely used [42].

Contact materials are used to ensure a good electrical connection between the interconnect and the cell [34,62]. Nickel mesh is widely used on the fuel side [62,63]. These provide high electrical contact, good gas distribution and stability during operation [12,64]. Perovskites are often used on the air side due to their good electrical conductivity and low cost in comparison to noble metal contacting [62,65,66]. During manufacturing, the contact layer can be applied either to the interconnector or directly to the cell [34].

2.2. Cell materials

The SOC consists of three main components: the fuel-side electrode, the air-side electrode and the electrolyte. The electrolyte is a solid oxide material that conducts the negative oxygen ions between the fuel-side

electrode and the air-side electrode. On the air-side electrode, another layer is often applied to act as a current collector layer (CCL) [34,65]. Together they will be referred to here as the air-side layers and the materials used will be referred to as the air-side materials. Similarly, the fuel-side electrode and the layer on top of it are referred to as the fuel-side layers and the materials are referred to as the fuel-side materials. A two-layer structure consisting of electrode and CCL can be used for the fuel-side layers and materials in ESCs. In FESCs, the fuel-side layers consist of the substrate and the fuel-side electrode.

Table 1 shows the cell materials used by various manufacturers. Due to the young age of the technology, the materials are very similar, with the greatest variation in air-side materials. On the air side, only perovskite-type materials with the formula ABO_3 or their composite with gadolinia-doped ceria (GDC) are used. The most common perovskite-type material is $La_xSr_{1-x}Co_yFe_{1-y}O_{3-\delta}$ (LSCF), followed by $La_xSr_{1-x}CoO_{3-\delta}$ (LSC), both of which are considered state of the art [34,67,68]. $La_xSr_{1-x}MnO_{3-\delta}$ (LSM), $La_1Mn_{0.45}Co_{0.35}Cu_{0.20}O_3$ (LCC10) and $La_{0.97}Mn_{0.4}Co_{0.3}Cu_{0.3}O_{3-\delta}$ (LCC12) are also used. However, LCC10 and LCC12 are exclusively used as CCL [69,70]. LSM, on the other hand, is an electrode material that was widely used in the past but has been replaced by LSC and LSCF due to their superior performance [67,71]. However, LSM is chemically more stable when used with stabilized zirconia as the electrolyte [29,67]. LSCF and LSC require a reaction barrier between the stabilized zirconia, which is usually made of GDC [72–74].

Stabilized zirconia is the most commonly used SoA electrolyte

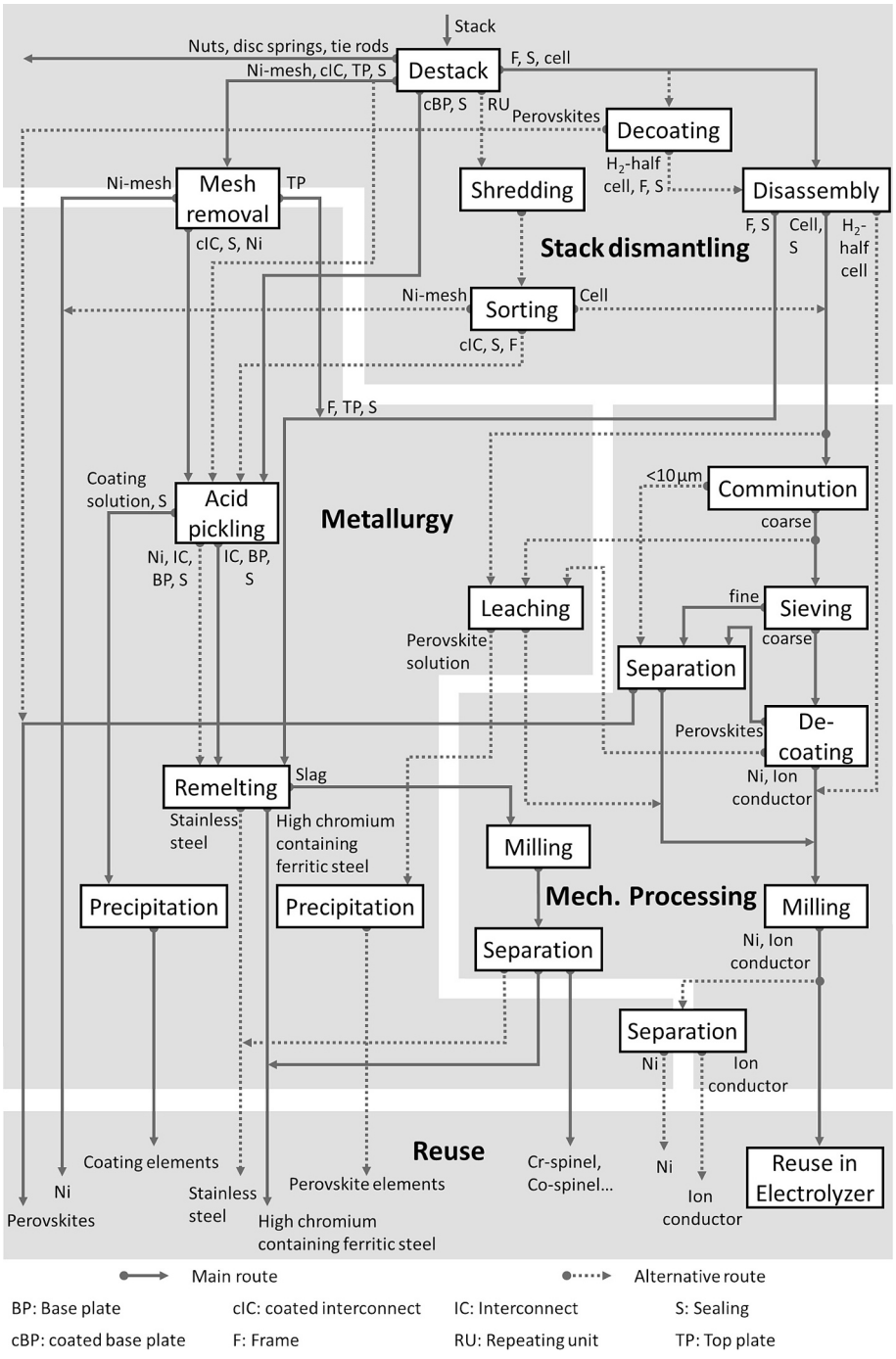

Fig. 2. SOC stack recycling process chain with main stages of dismantling, mechanical processing, metallurgy and reuse.

[34,67]. As can be seen in Table 1, yttria-stabilized zirconia (YSZ) is primarily used for FESCs. There is more variation in ESCs. In addition to YSZ, materials with higher ionic conductivity are used, such as scandia-stabilized zirconia (ScSZ), scandia-based stabilized zirconia or ytterbia-stabilized zirconia (YbSZ) [29,75,76].

The fuel-side layers of all the manufacturers considered here consist of a Ni-ion conductor cermet, which corresponds to the SoA [34,77]. In the case of FESCs, the ion conductor is YSZ, while for ESCs, GDC or samaria-doped ceria (SDC) is used. This is similar to the SoA as it is described in the literature [68,78].

3. Recycling process chain

Derived from the published recycling strategies [11,12] and with regard to the recycling chains of comparable systems, such as lithium-ion battery or e-waste recycling [79,80], a recycling chain consisting of three main processing blocks emerges: Stack dismantling, mechanical processing and metallurgy. In addition to these three main elements, the reuse of the recovered materials is also addressed.

Fig. 2 shows the proposed SOC stack recycling process chain. In the stack dismantling the SOC stack is separated into its macroscopic components. The separated metallic components are sent directly to the metallurgical processes and recycled into materials. The ceramic components, i.e., the cells, are mainly processed mechanically to liberate and separate the microscopically small material composites. Finally, reuse, where possibilities for direct reuse in SOELs (closed loop) as well as alternative applications (open loop) are discussed.

The recycling chain for SOC stacks is presented below, and individual key process steps are highlighted.

3.1. Stack dismantling

As described above, SOC stacks can be operated reversibly in fuel cell and electrolysis mode. SOELs and SOFCs have comparable components and materials. Therefore, both stacks are considered together for dismantling in the following. Al Assadi, et al. [17] point out that the main challenge in disassembling SOC stacks is the bonding of the individual components at the sealing areas. These joints are located between the layered components interconnect (IC) and frame, and also as a joint between the cell and frame [[50], here glass sealant]. This results in two essential process steps that are necessary for disassembly: (1) separation of the layers between the IC and frame and (2) separation of the cell from the frame. Other disassembly steps are not discussed in detail in this paper. These would include cutting and separating the nickel mesh. The requirement for all processes is an almost 100 % separation of the different materials with the aim of achieving the best possible recycling result. In the following, possible processes for both process steps (1) and (2) are presented and a prototype system is shown for each. An overview of the dismantling process chain, including the approaches presented below, with the resulting products and subsequent recycling paths is shown in Fig. 3.

3.1.1. Process step (1) – Separation of layers at joint IC - frame

The production of SOC stacks according to best available techniques can be associated with quite high manufacturing tolerances in terms of the amount and distribution of the glass sealant. This results in different component distances and limited points of attack for a cutting tool of the automated disassembly set-up. Fig. 4 shows the stack profile recorded by a laser profile sensor, characterized by the gaps between the stacked components. The gaps can be used as attachment points for disassembly. The brittle property of the glass sealant can be utilized for disassembly. Nevertheless, high process forces are required.

To select possible separation processes, the methodology form DIN 8580 [81] and DIN/TS 54405 [82] can be applied. For (1), mechanical processes such as cutting, machining or abrasion are particularly suitable. As both joining partners are solid steel components, peeling or stretching can be excluded. A prototype system for the splitting and wedge-cutting process is analyzed and constructed as a representative solution (Fig. 5). A wedge is used as the cutting tool. The wedge geometry (tip, length and angle) has been dimensioned to enable complete separation of the upper layer with one wedge and one movement. For height positioning, a spring plunger with position sensing by means of an actuating bolt is used to mechanically locate the gaps between the stacked components. Alternatively, a laser profile sensor may be used to identify the correct position without contact (cf. Fig. 4). The energy is applied via pneumatic cylinders. A linear axis is used to adjust the height of the separating system. The process enables component-specific separation. Due to the high energy input, small cracks my appear in the cells.

3.1.2. Process step (2) – Separation of cell and frame

The experimental cell (dimension approx. 200 × 200 mm) is brittle and is fixed to the frame on all sides with glass sealant. The challenge during separation is to remove as much of the cell material as possible.

Mechanical processes such as cutting and chiseling may be considered for separation. A prototype system for a stamp-out process with a die cutter is being investigated and therefore constructed as a representative solution (Fig. 6). The cutting tool is an additively manufactured die with inserts on the bottom. The force is applied by a pneumatic cylinder. The frame is positioned under the stamp using end stops. The process forces are significantly lower than in process step (1). Validation studies have demonstrated over 99 % recovery of cell material (illustrated in Fig. 7). This was measured by determining the mass of the separated cell material and the mass of the cell fragments still attached

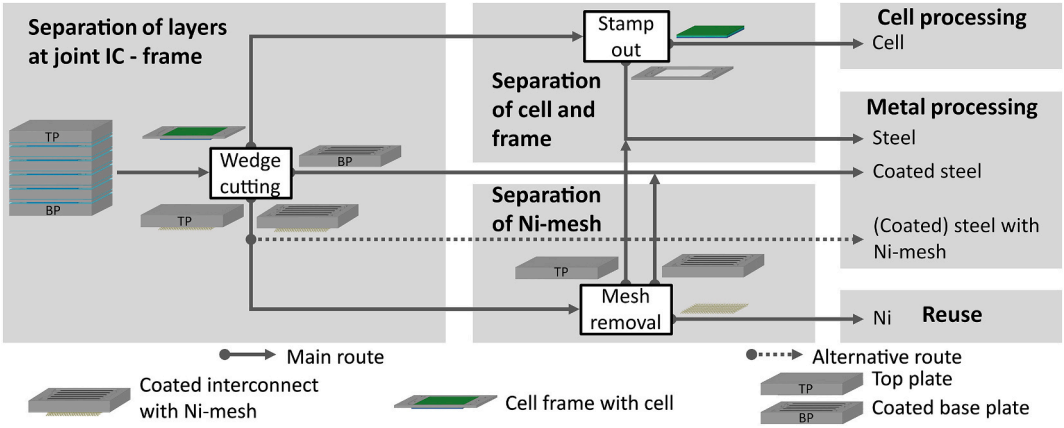

Fig. 3. Process scheme for the SOC stack disassembly.

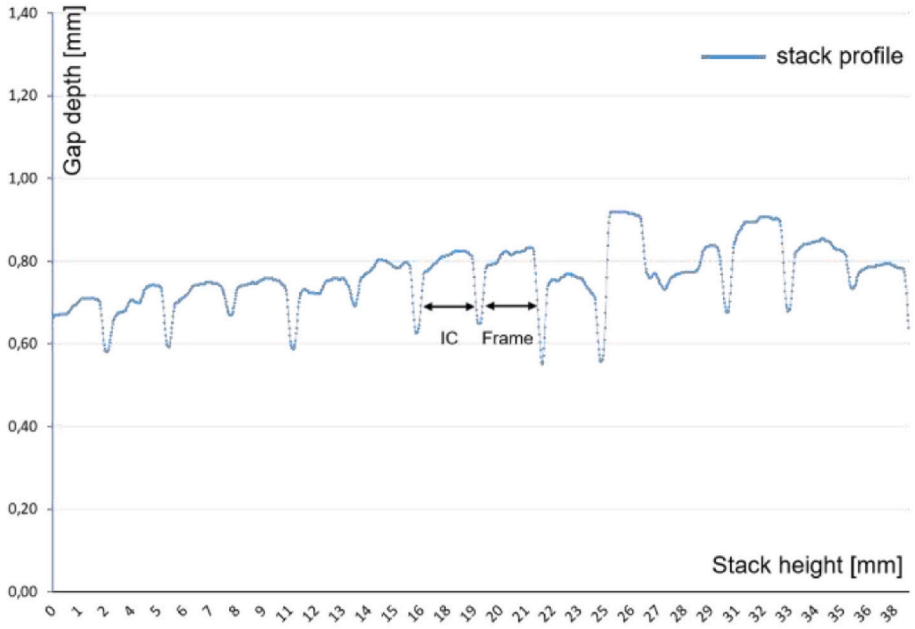

Fig. 4. Recorded stack profile using laser profile sensor. IC and frame are both approx. 3 mm thick. Gaps are less than 1 mm wide and can vary.

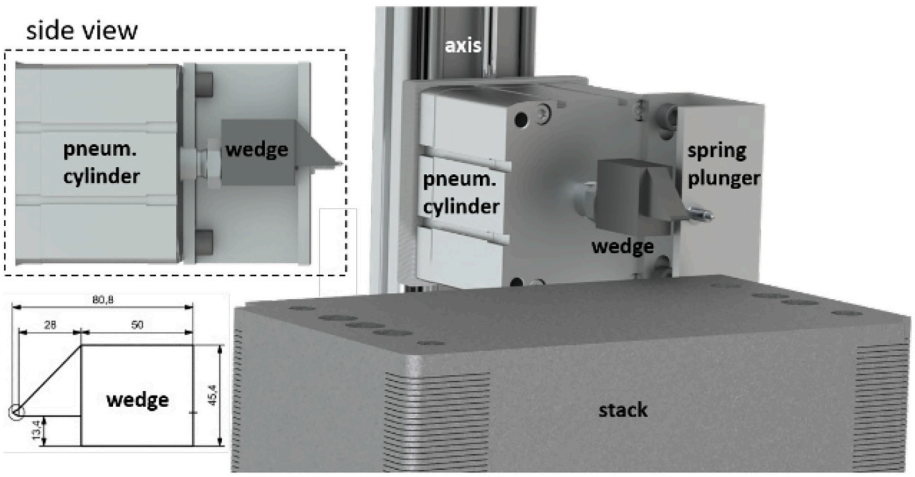

Fig. 5. Prototype system for separating IC and frame via wedge cutting.

to the frame by weighing. Fig. 7 shows the result after process (2). Fragments may remain on the frame (see top left).

The two methods prove the fundamental feasibility of automated and material-specific disassembly of SOC stacks with respect to the targeted joints.

3.1.3. *Mechanical processing of stacks and stack components*

As an alternative to disassembly, stack components can be mechanically processed. In mechanical processing, the components are shredded into particles, ideally consisting of one class or type of material. The finer-grained and firmer the different materials are combined, the more complex the shredding process and the smaller the final liberated particle size of the product. Mechanical processing is more flexible than disassembly and does not need to be redesigned or adapted for each new type of electrolyzer. However, comminution produces more fine particles and is more energy intensive. Furthermore, the stack, which consists of multiple layers of mainly steel and is encased in robust steel end plates, exhibits the characteristics of a solid steel cube. Consequently, comminution of an entire stack is not a viable option. In order to mechanically process an entire stack, the steel parts of the stack would have to be very thin while being able to withstand the high pressures, forces and temperatures of the high-temperature electrolyzer in operation.

Depending on the success of the disassembly in separating the individual layers of the stack, layers may still be connected or remnants may remain after disassembly. The effort required to separate these layers by shredding depends on the materials, connections and dimensions of the layers. To illustrate, the ceramic cell is highly brittle and can be reliably and rapidly separated from ductile steel frames. In the best case, this requires only about 0.02 kWh/t of energy (experiments on the above-mentioned experimental cell using kinetic impact). The steel frame remains intact and shows only deformations.

In contrast, nickel meshes and interconnects are often strongly bonded together, for example by many soldered and sintered joints, and are challenging to separate from the remaining parts. Ductile layers tend to wrap around each other under stress rather than separating from each

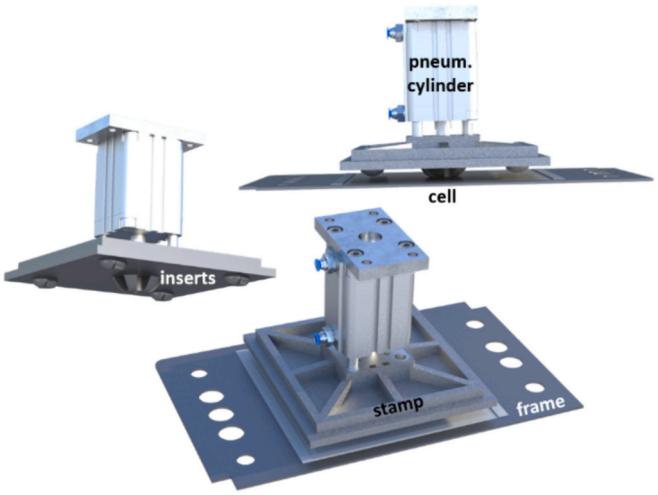

Fig. 6. Prototype system for separating cell and frame via stamp with inserts.

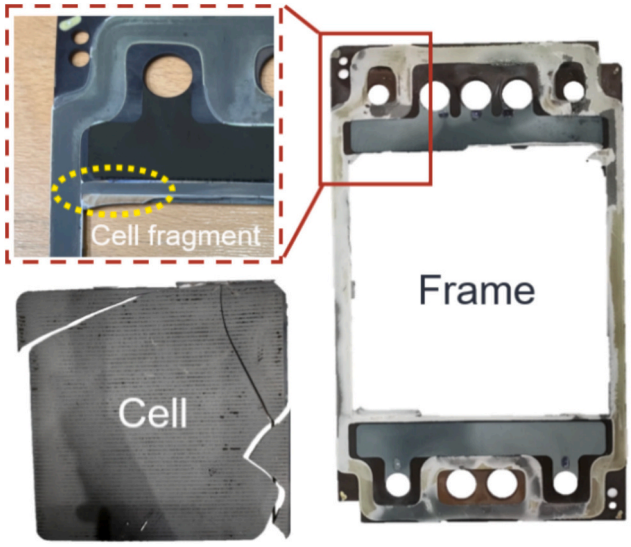

Fig. 7. Cell material separated from the frame.

other. Therefore, to mechanically liberate these materials, the entire layer of steel and nickel mesh must be cut and shredded into small particles in an energy-intensive process.

Physical sorting of a mixture of ferritic steel, nickel and cell material, which also contains a high proportion of nickel, is complex because the separation properties of the three materials, such as density and magnetism, are either too similar or outside the scope of conventional separation processes. It is therefore preferable to apply sensor-based sorting techniques. Optical sensors can detect the material of particles based on their color and spectroscopic reflectance profile. However, optical sensors are susceptible to material changes and require optimization for a narrow range of possible particles. Therefore, the best option is to prevent the mixing of the different materials: Layers can be separated by disassembly to prevent their materials from mixing during joint processing.

3.2. Cell processing and reuse of cell materials

The previous stack dismantling resulted in completely separated SOCs that can be directly used as input for cell material processing. The state of the cell can be either in one piece or, more likely, broken into several centimeter-sized fragments. Cell processing primarily involves mechanical processes to liberate and separate materials from the microscopic composite structures used in SOCs.

The processing of the cells can be divided into two basic steps: (1) liberation and separation of the perovskites and (2) processing of the remaining cell, i.e., the ionic conductors and nickel. An overview of processes for carrying out these two steps is presented below and illustrated in a process scheme in Fig. 8. The most promising of these processes are discussed in greater detail in the subsequent chapters.

3.2.1. Process step (1) – Liberation and separation of perovskites

There are a number of approaches to liberate and separate the perovskite materials. In this study, a combination of selective comminution followed by selective decoating of the cell particles is considered as the main route (Fig. 8). In this route, the cells are first coarsely crushed to homogenize the material and prepare it for the decoating step. Selective comminution is achieved by preferential breakage of the perovskite material. This allows the separation of a first pre-concentrate of perovskites in a subsequent sieving process after comminution. The pre-concentrate is subjected to a separation stage to recover the perovskites based on differences in physical properties. Suitable separation processes are discussed in chapter 3.2.2. The coarse particles resulting from the sieving still contain perovskites that have been deposited on the surface as a fine powder or are still present on the cell as a composite layer. These perovskites can be selectively separated and recovered using a particle decoating process. The process of mechanical decoating is the subject of chapter 3.2.1, where particle decoating is discussed in more detail. Prior to reuse, the perovskites must be purified in a separation process. The remaining material of the cell is particles consisting of the ceramic ionic conductors, i.e., YSZ and GDC, as well as nickel. Both selective processes in this approach produce pre-concentrates or almost pure products that make subsequent separation less complex. Moreover, due to the comminution, this process is independent of the condition of the cell, whether it is broken or not, and the geometry of the cells, i.e., size, shape. It is also possible to work with fewer or no additional hazardous substances compared to alternative processes.

An alternative approach to particle decoating is the surface decoating of entire cells. In this process, the perovskite layers are selectively removed by targeted stress. Consequently, the orientation of the cell is crucial for the targeted stressing process, which makes handling more challenging in case of cell breakage. For this reason, this process should be initiated as soon as the perovskite layers are accessible, as illustrated in the complete recycling chain (Fig. 2), to prevent breakage due to the separation of the cell from its frame. Two potential processes have been proposed: mechanical scratching followed by polishing or leaching, as presented by Saffirio, et al. [18] and Yenesew, et al. [19], and ultrasonic decoating, as illustrated by Kaiser, et al. [21]. These surface decoating processes can achieve a high degree of selectivity, allowing the recovery of high-purity products, as demonstrated by Kaiser, et al. [21]. Since the separated layers are not chemically altered, direct reuse could be a viable option as long as the stoichiometry and material are uniform and there is no operational contamination. Despite the potential of surface decoating, it remains constrained to cells that are as undamaged as possible, which may limit its applicability in an automated de-mounting and disassembly process. Therefore, this process is only considered as an alternative route.

Selective leaching is another approach that competes with decoating. While the discussed decoating processes mechanically separate the perovskite layers, the leaching process selectively dissolves the layers chemically. Selective leaching of the perovskites also involves an upstream oxidation of the metallic nickel present in the cell, as nickel oxide has a higher stability against inorganic acids [20]. The oxidation can be carried out at the end of the stack lifetime and is not an additional step, as the nickel oxide is required anyway before reuse in SOCs. Leaching can treat intact or broken cells as well as pre-crushed cell particles. This process produces high-purity products and is also suitable for scale-up as shown by Sarner, et al. [20]. In a recent study, Sarner, et al. [83]

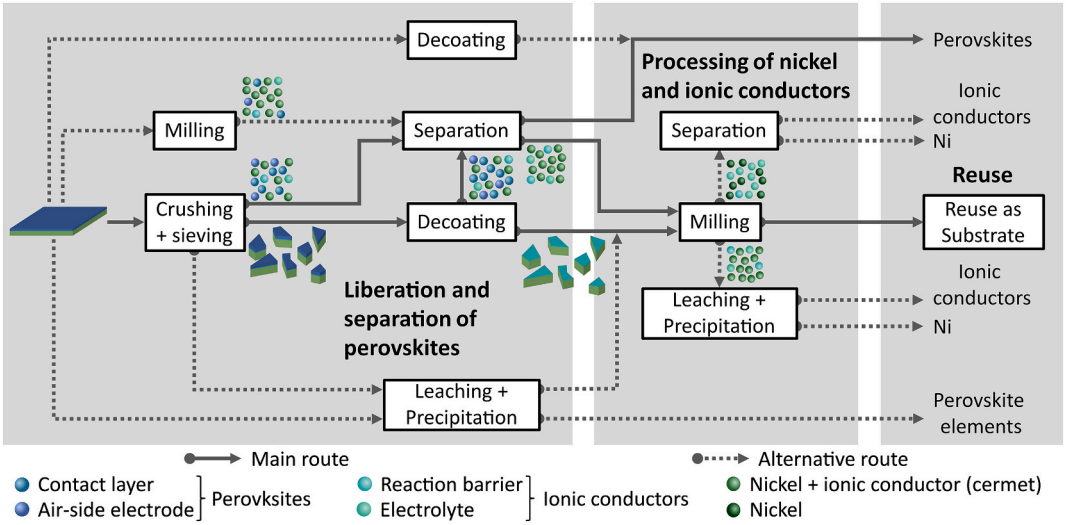

Fig. 8. Process scheme for the cell processing.

demonstrated that complete separation of the perovskites is achievable through leaching, yielding a solution with over 97 % purity. Moreover, they were able to recover more than 97 % of the remaining solid fraction (NiO and ionic conductors) with a purity of more than 99 % [83]. However, leaching requires additional hazardous substances that must be safely disposed of or recycled. Furthermore, the elements originating from the perovskite must be selectively recovered in a downstream process step and can be reused as a raw material [83]. Due to the hazardous materials used and the complexity of this approach, mechanical processes are preferred as long as they meet the purity and stoichiometry requirements for reuse in SOC production. However, leaching of the concentrate from the mechanical recycling could also be considered in order to further purify the product.

The final option is a process that is typically employed for finely intergrown materials. In this process, after the dismantling stage, the cell is directly subjected to crushing and milling until the target materials are completely liberated, resulting in single-digit micrometer range particles and smaller. The liberated particles can then be recovered by wet chemical methods based on their physical properties, particularly surface properties. As presented by Ahn, Rudolph [84], liquid-liquid particle separation is one of the potential methods to recover sub-micron particles from the electrolyzer cells based on their wettability differences. Since the surface energy of the critical raw materials utilized in the SOC is commonly high, additional reagents are required to hydrophobicize the particles for selective separation. For that reason, the probability of selective separation depends on the interactions between each solid particle, the liquid, and the reagent mixture used. In the case of perovskite recovery, so far this process is not regarded as an optimal solution. The perovskites are not finely intergrown; rather, they are already spatially separated and only intergrown with the other materials in a plane. Therefore, it can be assumed that this process requires more effort to achieve the desired result compared to the case where the selectivity of comminution is already used for enrichment. Furthermore, additional chemicals are required to achieve the desired selectivity of particle separation in liquid phases.

3.2.2. *Process step (2) – Processing of nickel and ionic conductors*

The treatment of ionic conductors and nickel exhibits less variety in the literature to date than that of perovskite separation. The first option is primarily applicable to FESCs. As already described by Sarner, et al. [20], the fuel side, electrolyte and GDC can be milled together and this mixture can be used as a substrate in new FESCs with the addition of pristine material. Although this is an elegant solution as the direct reuse of the material mixture eliminates the need to separate nickel from the ionic conductors, GDC will dissipate into the substrate and accumulate over time with repeated cycling.

An alternative is to finely mill the material and then separate the nickel from the ionic conductors. There are two approaches to separation. One approach uses acid for leaching. The powder can either be leached directly after grinding, as described by Yenesew, et al. [19], or first undergo hydrothermal treatment to further disaggregate the Ni-YSZ cermet prior to the leaching, as described by Saffirio, et al. [18]. Using this approach, Yenesew, et al. [19] were able to recover over 89 % of the YSZ and over 91 % of the NiO, both with a purity of around 99 %. On the other hand, Saffirio, et al. [18] achieved an estimated recovery for NiO and YSZ of approximately 90 % [85], with a YSZ purity of over 99 %. The other approach to the separation of nickel and ionic conductors is to use separation concepts based on the physical properties of the materials. This approach requires complete mechanical liberation through comminution in order to be able to separate the materials.

A current gap in the recycling chain is the separation of different ionic conductors. In the case of FESCs, this is the separation of YSZ and GDC. In terms of mass, GDC represents only a small fraction of the YSZ used, and in small quantities, GDC is not expected to affect the functionality of the YSZ if not used as a thin film electrolyte [19,20]. Therefore, GDC is often overlooked in FESC recycling, but it is inevitably a concern due to the scarcity of these elements. For ESCs, however, this could mean the separation of ScSZ from GDC and YSZ. At this point at the latest, it is crucial to implement suitable separation techniques to achieve a closed-loop recycling process and prevent the downcycling of these critical raw materials.

3.2.3. *Mechanical decoating*

Among the mechanical processes for liberating cell materials, decoating approaches are particularly promising, as they have the potential to recover materials from layered structures with high purity [21]. For the sake of simplicity, the layer to be removed will henceforth be referred to as the top layer. In the simplest scenario of mechanical decoating, the stress is applied only to the top of the layered structure, with the removal process being largely influenced by the process parameters and the properties of the top layer itself. This means that the specific differences in material properties within the layered structure do not significantly affect the removal process. One process that could be assigned to this category is grinding. The thickness and hardness of the top layer, as well as its connection to the second layer, are relevant for the removal during the grinding process and determine the type of grinding medium to be employed, the required grinding time and the optimal grinding speed. However, this means that the removal process is

not necessarily selective for the top layer, especially in the case of an uneven layer structure. Consequently, either residual material remains on the surface or the underlying layer is partially removed. This was also observed by Saffirio, et al. [18]. In their process, polishing was used to remove perovskite residues and the reaction barrier. However, when the cross section was examined, it was found that in addition to the reaction barrier, all of the underlying electrolyte had been removed. If the previously separated air-side electrode together with the product of the polishing step were considered as a perovskite concentrate, the purity would only reach an estimated 50 % based on the cells used. Therefore, the lack of selectivity for the layer to be removed in the process resulted in a product with a lower degree of purity.

The selectivity for the top layer can be increased by the application of processes related to material and mechanical properties. In the event that the top side remains the sole target of the stress, it is necessary that at least the layer underneath the top layer exhibits a greater stability against stress than the top layer. By adjusting the stress parameters, it is possible to ensure that the top layer is removed without destroying the layers underneath. This phenomenon is exploited in the ultrasonic surface decoating process. Kaiser, et al. [21] demonstrated, that this approach can achieve high selectivity and the production of high-purity materials for the separation of perovskite layers from SOCs. Their findings demonstrated that ultrasonic decoating has the potential to fully recover perovskite layers on the air side with a purity of up to over 99 %. This indicates that further purification processes may not be necessary, as two pure product streams are generated. In theory, the process could also be automated, given the high selectivity for the material. However, it is important to note that the application of this process depends on the alignment of the cell with respect to the sonotrode. Given the thin, highly brittle nature of SOCs, there is a high probability that the cell will break during upstream dismantling. This, in turn, restricts the applicability of ultrasonic surface decoating, as the alignment of all fragments can be challenging.

In order to overcome this challenge, it is essential to develop an effective decoating process that does not depend on the orientation of the cell with respect to the acting stress, i.e., that all surfaces are potentially stressed. To still achieve material selective decoating under these conditions, it is necessary to consider the material and mechanical properties of all layers. Differences in properties between the layers can lead to a selectivity of a comminution process. In order to achieve the desired selective detachment of the top layer, i.e., decoating, it is necessary that the top layer exhibits a lower stability to the selected stress than the other layers. This type of decoating can be considered a case of selective comminution. Here, the material is mainly separated from the surface, particularly from the top layer, and there is no or little comminution by fracture perpendicular to the layer structure. Therefore, the material from the top layer accumulates in the fines and can be separated by classification. This breakage mechanism is called abrasion and requires low stress intensity [86,87].

In this study, ultrasonic decoating of cell particles is proposed for the recycling of SOCs. The method based on ultrasonic surface decoating as presented by Kaiser, et al. [21] (cf. Fig. 9a) is now applied to cell particles, whereby particles of the cell instead of whole cells are exposed to the sonotrode (cf. Fig. 9b). In this process, the particles can move freely in the liquid, so that the ultrasound-induced stress affects the entire surface of each particle. The size of the cell particles is therefore very important for their free movement and later removal in the classification step. After dismantling, it can be observed that the cell consists of fragments of varying sizes. Consequently, an additional upstream comminution step for cells is necessary to prepare them for the decoating step. This comminution step must be suitable for the high brittleness and hardness of the material.

One comminution process that fulfills these requirements is a ball mill. First results of a comminution of cells in a ball mill have demonstrated that this process also leads to a selective comminution [88]. The resulting fine particles (≤100 µm) can be recovered as a first concentrate of perovskites, with up to 75 % of the perovskites recovered after a sieving step (cf. Fig. 8). The coarse particles (>100 µm) are mostly platelet-shaped and have a reduced perovskite content (cf. Fig. 9c). After sieving, the coarse particles are cleaned of residual perovskite by ultrasonic decoating (cf. Fig. 9d). Initial tests conducted under conditions comparable to those employed by Kaiser, et al. [21] have already demonstrated the potential efficiency of ultrasonic particle decoating. Overall, more than 97 % of the perovskite was recovered with a mass fraction up to more than 50 %. The remaining materials can be recovered up to 90 % with a residual perovskite mass fraction of less than 0.5 %. Despite being less selective than surface decoating, particle decoating still achieves high recoveries. Furthermore, it offers significant advantages for an automated approach due to its greater flexibility. Nevertheless, additional research and effort is required to optimize the process, particularly with respect to the upstream comminution and process parameters.

3.2.4. Separation

The fine concentrate from the previous mechanical steps consists of high-value particles in the sub-micron to few microns range. As defined in many publications, particles in this size range (below 10 µm) are often referred to as ultrafine particles in mineral processing [89–91]. The resulting high-value particles cannot be considered mechanically recovered in practice, as they contain a mass fraction of impurities of up to more than 50 %. Chemical methods, such as leaching, pyrometallurgy or hydrometallurgy may be advantageous to improve the efficiency, but

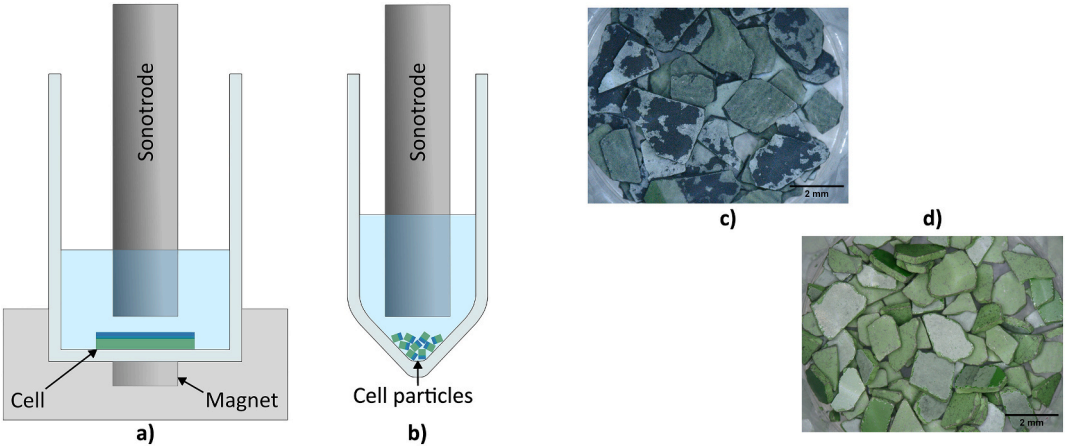

Fig. 9. a) Experimental setup for ultrasonic surface decoating and b) experimental setup for ultrasonic particle decoating with corresponding images for particles c) before ultrasonic stressing (dark = perovskites) and d) after 40 s of stressing.

result in high energy consumption compared to the physical processes. As a compromise between metallurgical treatments and milling processes, particle technology based on wet chemical methods is widely used to separate the valuable ultrafine fractions [92]. Especially, the investigations based on the surface and magnetic properties of the particles provide a potential for recovering valuable minerals from SOCs, as shown in Fig. 10.

Hydrophobicity is one of the physicochemical surface properties that plays an important role in the separation of ultrafine particles by froth flotation and liquid-liquid microparticle separation (LLPS) [93]. The effectiveness of utilizing the wettability of the particles for recycling precious secondary raw materials is currently being investigated. For instance, the representative materials of the proton exchange membrane electrolyzer were selectively separated by LLPS with over 97 % recovery [84], and the froth flotation was applied to recover lithium metal oxides and graphite from batteries with a recovery over 96 % [94].

The materials used in SOCs are metal oxides which are intrinsically hydrophilic, therefore, selective separation can be achieved through hydrophobizing the particles using surfactants. In the previous work from Ahn, et al. [95], the low water contact angles of the pristine particles of NiO, LSM, ZrO_2, and YSZ confirmed that the materials have high surface energy. A notable surface characteristic was their surface charge, which changes with the pH of the dispersion. When dispersed in an alkaline solution, the surface charges of the mentioned materials are divided into two groups: positively charged (electrode materials) and negatively charged (solid electrolyte materials). The wettability of the positively charged particles can be altered by interacting with the surfactant molecules, which have negatively charged polar head groups. As amphiphilic molecules, surfactants contain hydrophilic heads and lipophilic tails. Once the surfactant molecules are fully adsorbed onto the target colloidal particle, the hydrophobic tails of the surfactant are directed away from the particle, i.e., the particles are hydrophobized. The LLPS allows the selective separation of particles with different (de) wetting behavior with high recovery [96,97]. The LLPS system contains an organic phase, an aqueous phase, colloidal particles and reagents. According to the previous work of Ahn, Rudolph [84], the separation process was designed using cyclohexane as the organic phase and sodium dodecyl sulfate (SDS) as the surfactant, demonstrating the potential of the LLPS for SOC recycling. This system is highly influenced by pH, surfactant type and concentration, and agitation conditions, so the maximum recovery of the materials could be up to 70 %. Additionally, LLPS has mainly been applied in binary particle systems and rarely in systems containing more than four materials. For that reason, further investigations are required, focusing on a deep understanding of the particle-particle, particle-liquid, and particle-surfactant interactions.

Recently many studies have presented the possibility of recycling rare earth elements by exploiting their magnetic properties [98–100]. The alternative process to separate air-side materials such as LSCF, LCC10, or LSM from the particle mixture is magnetic separation. In order to characterize their magnetic properties, the response of intrinsic particles to a magnetic field has been studied. The magnetic susceptibilities ($\chi \cdot 10^{-4}$) of these air-side materials were above +1, supporting their paramagnetic properties. On the contrary, YSZ behaved like a diamagnetic material and NiO confirmed its antiferromagnetic behavior. Hence, magnetic particle removal through a high gradient magnetic separator (HGMS) can be a potential method. The purpose of using HGMS is to remove paramagnetic materials from diamagnetic or antiferromagnetic materials by capturing them in the magnetic matrix (cf. Fig. 10). This ferromagnetic matrix produces strong magnetic forces due to high field strength and high field gradients and is capable to capturing even weak magnetic particles [101]. However, the strength of the magnetization depends on the chemical composition of the feed material, which requires precise characterization of the feed material [102,103].

3.2.5. *Reuse of cell materials in new SOCs*

Reuse of recovered ceramic powders for the manufacturing of new SOCs is likely the most sustainable approach and should be targeted (closed loop). Nevertheless, the powders must meet specific requirements tailored to their intended use. For FESCs, the removal of air-side materials is highlighted as initial step. For the majority of the remaining powder, different pathways may be applied subsequently. The requirements, limitations and advantages of each pathway are summarized in the following.

Electrolyte recovery: The input material must exhibit high phase purity, both narrow and fine particle size distribution, as well as sufficient sinterability. Phase purity is necessary to provide high ionic conduction (8YSZ ~ $8 \cdot 10^{-3}$ Scm^{-1}, GDC ~ $7 \cdot 10^{-2}$ Scm^{-1}, both at 700 °C [104]) while ensuring electronic isolation. YSZ-GDC composites are known to increase the activation energy for ionic conduction, potentially leading to an order of magnitude decrease in ionic conductivity [105]. Additionally, the presence of metallic nickel could lead to electronic leakage. Therefore, it is imperative to ensure the separation of Ni (O) and GDC from YSZ, assuming YSZ serves as the electrolyte material

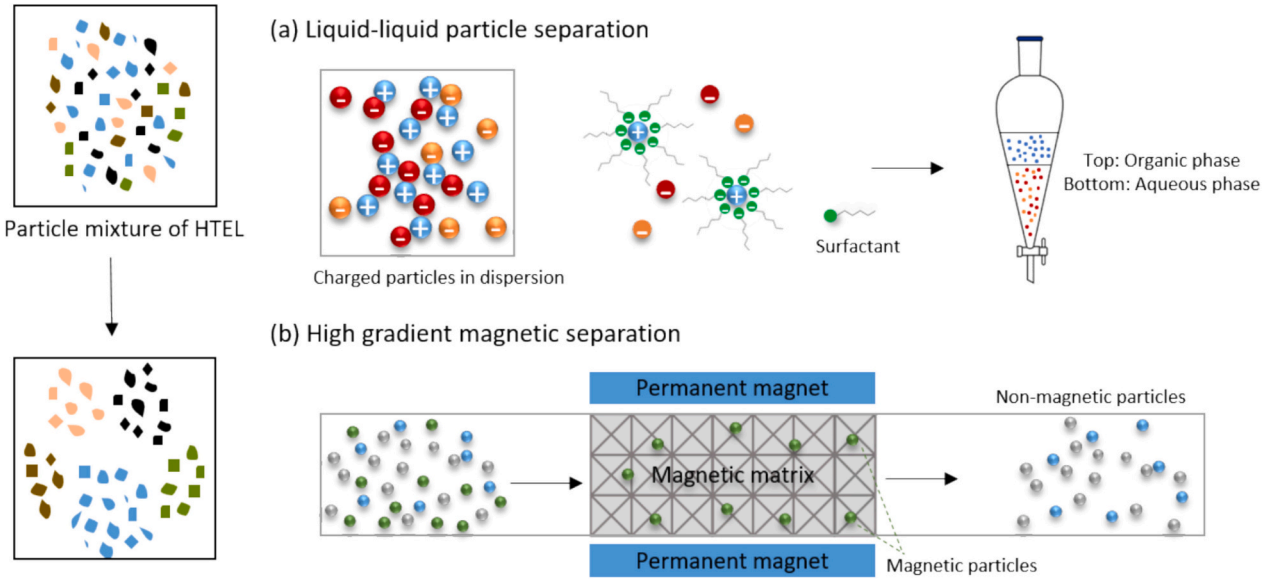

Fig. 10. Schematic diagram of mechanical separation processes for ultrafine particles.

in this scenario. Other impurities, such as silica, can impair the conductive properties to an even greater extend, even at low concentration levels of a few hundred parts per million [106]. Moreover, the particle characteristics strongly influence the sinterability of the ceramic. For 8YSZ electrolytes, feed material powders in the submicron range are chosen, typically having a specific surface area exceeding 17 m^2g^{-1}, thus ensuring the densification of the thin electrolyte layer [107]. Achieving a homogeneous particle size distribution in the submicron range requires high-energy grinding and sieving steps, or possibly even hydrothermal disintegration of the particle network [108]. Under these high stress conditions, the crystal structure of the tetragonal/cubic YSZ phase may deteriorate, which was observed by Saffirio, et al. [18]. The transformation to the monoclinic phase negatively affects the ionic conductivity as well as the thermal stability of the material. For these reasons, the processing of reclaimed ceramics as electrolytes is challenging. Since only small amounts of suitable material are required (~2 % of the total raw powder mass used for SOC manufacturing [50]), it is advisable to first consider alternative processing routes.

Fuel-side electrode: The reprocessing of SOC ceramic materials into fuel-side electrode powder entails similar challenges to those of electrolyte recovery. In contrast, Ni(O) must not be separated, while the homogeneous distribution of the Ni(O)-YSZ/GDC network is essential to increase the active area of the electrode/triple-phase boundary density. Changes in the Ni(O)-YSZ ratio are known to affect the microstructural evolution, such as pore volume fraction and triple-phase boundary length [109]. Additionally, it should be noted that 8YSZ with a low thermal synthesis history is typically used as the raw material for the manufacturing of both the fuel-side electrode and the electrolyte. For the manufacturing of the support layer, cheaper powder synthesis routes such as fused and crushed can be employed, because lower shrinkage rates are targeted in substrate manufacturing. The sinterability of the recovered powders is different depending on the thermal history and the quality of the pristine raw powders initially employed. The sintering conditions need to be adjusted in order to achieve dense and well-adhered functional layers for both electrolyte and fuel-side electrode. In general, the recovery into fuel-side electrode powder is slightly more favorable compared to electrolyte powder as there is no need for Ni(O) separation. However, separating GDC from ground cell material while maintaining Ni(O) integrity is challenging, and meeting purity requirements and suitable phase ratios will increase processing effort and cost.

Substrate recovery: As stated in the studies by Sarner et al. [12,20], substrate reprocessing may be the most superior option, especially considering the early stage of SOC market entry. The substrate serves as a mechanical support, providing electrical conduction and gas transport to the active cell area. Therefore, Ni(O) does not need to be separated and GDC traces should not hinder functionality as long as the mechanical stability is appropriately maintained in a reducing environment where Ce^{3+} tends to expand within the lattice [110]. Purity requirements are still of concern to provide longevity of the whole cell assembly, but trace element contamination is expected to be least critical in the substrate. Slight deviations in Ni(O): YSZ ratios are not a concern as long as the material is homogenized and a percolating Ni-YSZ-network can be formed. One significant advantage lies in the cost-effective processing of the particles into the micrometer range and the ability to tolerate variations in powder quality and composition: Mixtures of 3YSZ and 8YSZ (3 or 8 mol% of yttria in zirconia) are feasible, and the high thermal exposure of both the initial raw powder synthesis and the cell operating lifetime is less concerning, due to the desired final porous microstructure.

In addition to recovering the major cell components (YSZ, Ni(O), and GDC), attention should also be paid to the previously separated perovskite fraction, which contains critical materials like La, Sr, and Co (see Table 1). If mechanical separation can yield high-purity perovskites with unchanged stoichiometry, only the particle sizes need to be adjusted before incorporating the recycled perovskites into new oxygen electrode pastes. For use in new electrode pastes, it is necessary that the perovskite materials exhibit chemical uniformity. Ideally, the perovskite used in the oxygen electrode should chemically match the contact material used. Future studies are necessary to explore the material amount of recovered perovskite that can be incorporated into the initial raw powder to attain the desired sintering properties of the material. The direct reuse approach would be highly advantageous as it eliminates the need for further processing. If the material requirements cannot be met through mechanical separation, alternative recovery methods such as chemical processes must be considered. Alternatively, impure perovskites can be integrated into non-SOC-related applications.

3.3. Metal processing and potential reuse

As discussed in chapter 2, FESC SOC stack interconnects consist of metallic substrates with nickel meshes on the fuel side, spinel-based coatings and perovskite-based contact materials on the air side, and sealants along the edges. Crofer is the standard metallic substrate for JÜLICH, Fiaxell, Sunfire and Topsoe, with other SOC stack manufacturers also using similar ferritic steel variants (see Table 1). The widespread adoption of such ferritic steel-based interconnects allows for recycling via scrap remelting. However, for this route to be effective, it is crucial to understand the melt and slag compositions and how they vary with stack design and lifetime. Additionally, the element distribution to the melt, vapor and slag phases must be well understood to be able to adjust the final steel quality and produce high-quality alloys that meet existing market demands.

The recycling of JÜLICH SOC stack interconnects is used as a reference in the scheme shown in Fig. 2. Since most interconnects are based on ferritic steel, this approach can be broadly applied to other manufacturers as well. The proposed recycling route includes metallurgical and mechanical processes, namely (1) metal processing and (2) slag processing, respectively. These two process sections are illustrated in Fig. 11 and discussed in further detail below.

3.3.1. Process step (1) – Metal processing

In JÜLICH stacks, Crofer22APU/H is currently used as the preferred substrate due to its ability to form chromium-manganese spinel for enhanced chromium retention and Nb-containing Laves phase in Crofer22H for high creep resistance [111]. A recent study by Lastam, et al. [112] showed that an EoL JÜLICH F10 stack mesh-free interconnect consists of Fe and Cr, with less than 3.0 % (by weight) of trace elements, mainly Co and Mn. This composition is close to that of Crofer22 or similar AISI4xx ferritic steels, potentially enabling closed-loop recycling. However, it is important to note that this approach heavily relies on the successful separation of the nickel meshes from the steel. The meshes, which still have high nickel purity, could be dissected and reused as an alloying element in the production of nickel-containing alloys. However, as already mentioned in chapter 3.1, the complete mechanical removal of these meshes poses a challenge because they are soldered and/or sintered into the substrate, leaving behind nickel residues. Nickel is a trace element in Crofer22 alloys, with a maximum tolerance limit of 0.5 % (by weight) [113,114], and must therefore be minimized when remelting mesh-free interconnects. This requires further removal of the soldered nickel meshes, which can be accomplished by hot corrosion. This technique exploits the selective chemical reactivity of nickel to alkali sulfate salts when exposed to SO_3-containing atmospheres at high temperatures [115]. In this process, the interconnect is coated with the salts and exposed to elevated temperatures in a P (SO_3) atmosphere. This induces selective nickel dissolution, forming nickel sulfate-containing salt mixtures that can be dissolved in water after cooling, resulting in a nickel-free substrate.

Another challenge that may arise with scrap remelting is the presence of undesirable trace elements in the melt. Lastam, et al. [112] noted that cobalt from the MCF/MCO coatings tends to partition into the bulk

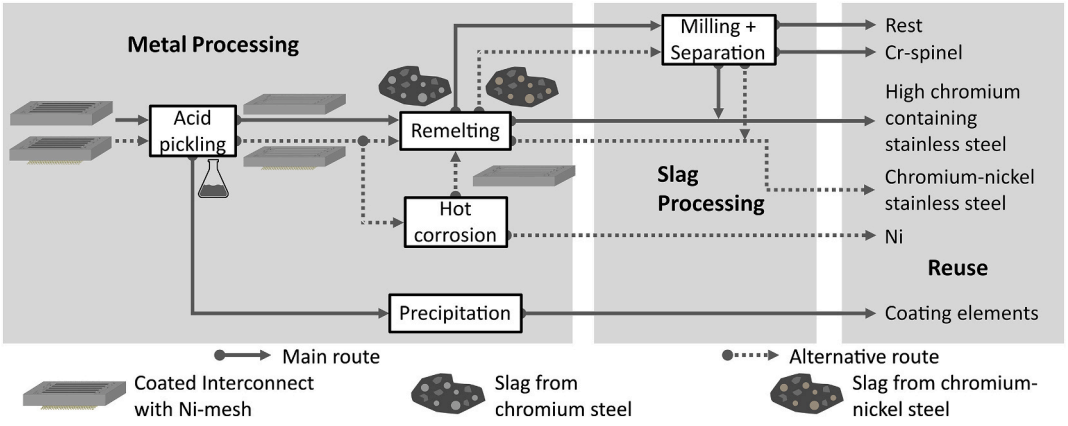

Fig. 11. Process scheme for the processing of metal parts of an SOC stack using the example of an interconnect assembly.

alloy rather than the slag phase. Since cobalt is considered an impurity in most ferritic steels [116], it must be controlled to a minimum level. This necessitates an interconnect decoating step prior to remelting, which can be achieved via chemical methods, such as acid pickling, or mechanical methods. As shown in the recycling scheme in Fig. 2 and Fig. 11, the acid pickling-precipitation route is proposed. Acid pickling is commonly used to remove oxide scale from steel surfaces and is preferred because of its selectivity for oxide layers, minimal substrate damage, and industrial scalability. The leached elements can then be subsequently recovered from the spent pickling liquor through precipitation. Mechanical decoating methods such as abrasive blasting and mechanical grinding are alternatives to pickling, but present difficulties in recovering the critical coating elements from waste materials that can be mixed with blasting or grinding media, and dispersed as airborne particles.

The processes described above can also be applied to the endplates. Conversely, the cell frames, typically composed of the same alloy but uncoated and without soldered nickel meshes, can be readily separated and refurbished for reuse or directly remelted into similar ferritic steels without significant contamination.

An alternative approach is open-loop recycling, in which the interconnects are transformed into alloys suitable for other applications. The addition of soldered nickel meshes increases the nickel content of the melt to 5–9 % (by weight), making it a potential feedstock for the production of AISI2xx and AISI3xx series steels. This route eliminates the need for prior nickel mesh removal. Preliminary studies by Lastam, et al. [117] demonstrated the feasibility of producing AISI304 stainless steel from the complete remelting of interconnects with nickel meshes, achieving a metal recovery of 95.7 %. Aside from minor alloying element additions, no blending with primary iron is necessary, allowing for a fully scrap-based steelmaking process.

3.3.2. *Process step (2) – Slag processing*

During remelting, the stack components are melted with fluxing agents and alloying elements under inert or reducing conditions to form a bulk alloy and slag. Slag formation is critical as it protects the melt from oxidation, limits the loss of alloying metal, and reduces impurities from the liquid metal. Slag typically floats on top of the molten metal since its density is less than that of the molten metal. The liquid slag and metal are cooled to ambient temperatures by either casting/air quenching or furnace cooling. Here, melting conditions are critical to selectively collect the impurities in the slag phase while maintaining a high metal yield. The solidified slag contains not only metal oxides as fluxing agents, but also oxidized metals and entrapped metals as inclusions from the alloy. Within these entrapped inclusions, some of the metals, particularly chromium, tend to oxidize easily and be lost to the slag phase and need to be preserved by optimizing the melt conditions or recovered in subsequent slag processing steps to maximize the recycling yield. It should also be noted that slags from different material streams can vary in composition, morphology and mineralogy due to different origins, metallurgical processes and cooling techniques. Therefore, slag systems need to be thoroughly characterized in order to identify the valuable target materials for recycling.

During the remelting of interconnect scrap, a considerable amount of Cr was detected in the slag, along with Fe and Mn and small amounts of Ni (likely from nickel mesh), Ti and Ba (likely from glass sealant) [117]. Slags from steel scrap recycling have relatively high Cr content (1–10 % by weight) [118], which is of high economic importance for the EU economy [119], thus, these slags can be considered as secondary raw materials for the recovery of Cr and other valuable elements. Besides, the slag mostly contains silicates such as monticellite and åkermanite. The main oxide phase in these slags is found to be spinel (AB_2O_4), which is the main host for Cr. It should be noted that spinel has a different composition in different slag samples. Spinel-forming elements are also found to be Al (in this case coming from fluxing agents used), Fe, Cr, Ni, and Mn; this finding is consistent with a previous study on the recyclability of the interconnect assembly by Lastam, et al. [112]. Spinel phases are considered to be chemically very stable; thus, it is challenging to apply leaching to extract Cr from the slag, which tends to favor mechanical processing because it is more feasible. Moreover, in pyrometallurgical battery recycling LiAl-spinels are used to recover Li from the slag phase, as this spinel has a 3-times higher Li content compared to most geogenic Li ores [120].

The mechanical processing route for recovering suspended metals, so-called metallic inclusions, from slags and high-value minerals involves slow cooling, crushing, grinding and sorting mainly by magnetic separation, gravity separation and flotation. Prior to size reduction of the slag, it is important to define the size of the target phases. Mineral liberation analysis has shown that slags from remelting trials indicate the presence of very fine Cr-rich spinel grains ($x_{50} < 45$ µm) within the matrix phases. In order to liberate these grains and achieve the desired particle size, a suitable mill is required based on the mechanical properties, namely hardness and brittleness of the slag. Such types of slags usually have a Mohs hardness between 5.5 and 6.5, as they mainly comprise silicates (Mohs hardness 5–5.5) and spinels (Mohs hardness 5.5–7). Based on these properties, ball mills and jet mills may be suitable for the desired size reduction of the slag materials. Kukurugya, et al. [118] applied magnetic and gravity separation techniques to the high Cr-containing stainless-steel slag and presented that these beneficiation methods show good potential for up-concentration (enrichment by a factor of 4), which can be beneficial for further alternative slag recycling processes such as hydrometallurgical processes. The separation recovery can be improved by slow cooling of the slag, which facilitates coalescence of metallic grains into larger droplets and the growth of Cr-bearing spinel to make physical separation easier. Rachmawati, et al. [120] characterized lithium-bearing slags with different cooling rates and

demonstrated that a lower cooling rate results in a coarser grain size of the target crystals. A larger grain size favors the liberation of the target phases from the slag during comminution, thereby improving the recovery during the separation process.

4. Conclusion and outlook

This study presented a first process scheme for the complete recycling of solid oxide stacks, with a particular focus on the FESC design. To this end, the most commonly used materials were compiled from data provided by manufacturers and literature sources. Based on these materials and the basic structure of an SOEL, processes from the disciplines of automated dismantling, mechanical recycling and metallurgy were presented with the holistic aim of recovering the majority of materials considered critical. In addition, reuse options were discussed and remaining challenges and gaps in the scheme were identified.

The feasibility of automated dismantling was demonstrated in principle, with initial approaches achieving high recovery rates for the individual components of the stack. The greatest challenges were encountered in the separation of the bonded components at the sealing areas. An existing gap is the separation of the nickel mesh from the interconnect, as these can be strongly connected. Mechanical shredding of entire stacks is considered difficult as it requires high energy input and separation of the individual materials is challenging as the usual separation characteristics are similar. Therefore, disassembly is the preferred option.

An overview of the recycling approaches for cell and metal processing of SOEL materials, as well as the recovery, purity achieved and remarks on their reuse, is presented in Table 2. As can be seen from the table, the majority of the existing approaches show high recoveries and/or purity levels. However, most of the recycled materials may require refinement prior to reuse as they have not yet been tested in new SOC applications. Therefore, further research is needed to investigate the reuse of recycled materials in new SOCs and to determine what proportions of recyclate in new cells will not degrade performance. It should also be noted that the recovery and purity values are from processes with a TRL less than five and are mainly based on unused or only tested cells. These values are thus not necessarily representative of an industrial scale, and it remains to be investigated how operation and aging of the SOC affect the recycling. Nevertheless, these approaches already provide useful starting points and serve as a conceptual basis for recycling.

Mechanical and hydrometallurgical processes represent the primary approaches for cell recycling. Compared to hydrometallurgical processes, mechanical processes offer the possibility of direct reuse of the materials and do not require additional hazardous substances, making them a preferred option. Moreover, mechanical processes have been shown to have the potential to achieve recoveries and selectivities comparable to those of hydrometallurgical processes. Promising processes include mechanical decoating, liquid-liquid particle separation and magnetic separation. However, it is important to note that these processes are still in the very early stages of development for application in cell recycling and require further research. The recycling of cell materials for reuse as electrolytes is considered as the most challenging among the various cell materials, due to the necessity of achieving high phase purity and the requirement for minimal impurities in the resulting material. Furthermore, no research has yet been conducted to date to investigate the separation of the different ionic conductors. Therefore, it is recommended that FESCs be processed into new substrate materials as their requirements are less stringent.

Metals recycling is a viable process and, in principle, the implementation of a closed-loop recycling system for used components is feasible. The issue of separation of the nickel mesh remains, as this would otherwise be incorporated into the metal phase, which would ultimately result in open-loop recycling, as also shown in Table 2. Reducing the strength of the bond between the mesh and the interconnect during stack manufacturing, for example by using fewer solder spots, may facilitate mechanical separation of these two components. Further research is required to develop effective decoating techniques for interconnects, with the aim of maintaining cobalt concentrations in the metal below the established limits. Another significant challenge is the recovery of materials in the slag phase. Its composition is highly complex and contains a considerable amount of Cr, particularly in spinel phases. These are regarded as chemically highly stable and necessitate mechanical processing. Mechanical recycling of electrolyzer slag still

Table 2
Overview of presented and compiled recycling processes for the main materials of SOELs, including the determined recovery rates and purities, as well as information for reuse.

Material	Recycling approach	Recovery in % (by mass)	Purity in % (by mass)	Remarks for reuse	Closed loop / open loop	Reference
Crofer steel with Ni-mesh	Remelting	~96	n/a	Refinement may be necessary	Open loop	[117]
Ni(O)	Leaching	90	n/a	In solution	Both	[85]
	Leaching	>91	~99	Reusable in substrates	Both	[19]
	LLPS	~70	~70	Study based on pristine material	Closed loop	Based on [95]
YSZ	After Leaching	90	>99	Refinement may be necessary	Both	[18,85]
	After Leaching	>89	~99	Refinement may be necessary	Both	[19]
	LLPS	~70	~70	Study based on pristine material	Closed loop	Based on [95]
Ni(O) + YSZ	After leaching	>97	>99	Reused in substrate	Closed loop	Based on [83]
	After surface decoating	~99	~99	Refinement may be necessary	Closed loop	Based on [21]
	After particle decoating	~90	~99	Refinement may be necessary	Closed loop	Own research based on [88]
Perovskites	Scraping + polishing	~100	<50	Refinement necessary	Closed loop	Estimation based on [18]
	Particle decoating	>97	~50	Refinement necessary	Closed loop	Own research based on [88]
	Surface decoating	~99	>98	Refinement may be necessary	Closed loop	Based on [21]
	Scraping	n/a	~99	Refinement may be necessary	Closed loop	Based on [19]
	Leaching	~100	>97	In solution	Both	Based on [83]

needs to be researched, but could be based on slag systems that have already been researched.

Overall, a preliminary framework for SOC stack recycling has been established. A significant portion of the materials involved are covered, and remaining gaps and challenges are identified. However, further research on the principal processes and optimization is still necessary. The investigations presented are based on independent materials, i.e., they do not originate from the same manufacturer or stack. Consequently, a comprehensive feasibility assessment of entire stacks is recommended. Furthermore, a life cycle assessment and a techno-economic assessment could be conducted to identify the preferred processes and those in most need of optimization.

CRediT authorship contribution statement

Carlo Kaiser: Writing – review & editing, Writing – original draft, Visualization, Methodology, Investigation, Conceptualization. **Sohyun Ahn:** Writing – review & editing, Writing – original draft, Visualization, Investigation. **Martin Brünner:** Writing – original draft, Investigation. **Dominik Goes:** Writing – original draft, Visualization, Investigation. **Jeraldine Lastam:** Writing – original draft, Investigation. **Shine-Od Mongoljiibuu:** Writing – review & editing, Writing – original draft, Investigation. **Stephan Sarner:** Writing – review & editing, Writing – original draft, Investigation. **Alexander Specht:** Investigation. **Jürgen Fleischer:** Supervision, Resources, Funding acquisition. **Norbert H. Menzler:** Writing – review & editing, Supervision, Resources, Funding acquisition. **Michael Müller:** Supervision, Resources, Funding acquisition. **Martin Rudolph:** Writing – review & editing, Supervision, Resources, Funding acquisition. **Bernd Friedrich:** Supervision, Resources, Funding acquisition. **Olivier Guillon:** Supervision, Resources, Funding acquisition. **Ruth Schwaiger:** Supervision, Resources, Funding acquisition. **Urs A. Peuker:** Writing – review & editing, Supervision, Resources, Project administration, Funding acquisition, Conceptualization.

Declaration of generative AI and AI-assisted technologies in the writing process

During the preparation of this work the authors used DeepL in order to improve the language and readability. After using this service, the authors reviewed and edited the content as needed and take full responsibility for the content of the publication.

Declaration of competing interest

The authors declare that they have no known competing financial interests or personal relationships that could have appeared to influence the work reported in this paper.

Acknowledgements

The authors acknowledge the financial support by the German Federal Ministry of Education and Research (BMBF) within the project “ReNaRe – Recycling – Nachhaltige Ressourcennutzung” under grant numbers 03HY111A, 03HY111B, 03HY111D, 03HY111E and 03HY111J. The authors would also like to thank the Forschungszentrum Jülich for their material support. The authors would also like to thank Anwar Al Assadi and Basile Thierry for their contribution to the results presented here.

Data availability

Data will be made available on request.

References

[1] IEA, Energy Technology Perspectives 2020, IEA, Paris, 2020.
[2] A. Millot, N. Maïzi, From open-loop energy revolutions to closed-loop transition: what drives carbon neutrality? Technol. Forecast. Soc. Chang. (2021) 172, https://doi.org/10.1016/j.techfore.2021.121003.
[3] X. Luo, J. Wang, M. Dooner, J. Clarke, Overview of current development in electrical energy storage technologies and the application potential in power system operation, Appl. Energy 137 (2015) 511–536, https://doi.org/10.1016/j.apenergy.2014.09.081.
[4] M.M. Rahman, A.O. Oni, E. Gemechu, A. Kumar, Assessment of energy storage technologies: a review, Energy Convers. Manag. (2020) 223, https://doi.org/10.1016/j.enconman.2020.113295.
[5] M.A. Rosen, S. Koohi-Fayegh, The prospects for hydrogen as an energy carrier: an overview of hydrogen energy and hydrogen energy systems, Energy Ecol. Environ. 1 (1) (2016) 10–29, https://doi.org/10.1007/s40974-016-0005-z.
[6] M. Yue, H. Lambert, E. Pahon, R. Roche, S. Jemei, D. Hissel, Hydrogen energy systems: a critical review of technologies, applications, trends and challenges, Renew. Sust. Energ. Rev. (2021) 146, https://doi.org/10.1016/j.rser.2021.111180.
[7] IEA, Global Hydrogen Review 2023, IEA, Paris, 2023.
[8] I. Rolo, V.A.F. Costa, F.P. Brito, Hydrogen-based energy systems: current technology development status, opportunities and challenges, Energies 17 (1) (2023), https://doi.org/10.3390/en17010180.
[9] M. El-Shafie, S. Kambara, Y. Hayakawa, Hydrogen production technologies overview, J. Power Energy Eng. 07 (01) (2019) 107–154, https://doi.org/10.4236/jpee.2019.71007.
[10] R.S. El-Emam, H. Özcan, Comprehensive review on the techno-economics of sustainable large-scale clean hydrogen production, J. Clean. Prod. 220 (2019) 593–609, https://doi.org/10.1016/j.jclepro.2019.01.309.
[11] A. Valente, D. Iribarren, J. Dufour, New end-of-life technologies applicable to FCH products, in: European Commission, CORDIS EU Research Results, 2018, https://doi.org/10.3030/700190.
[12] S. Sarner, A. Schreiber, N.H. Menzler, O. Guillon, Recycling strategies for solid oxide cells, Adv. Energy Mater. 12 (35) (2022), https://doi.org/10.1002/aenm.202201805.
[13] A.M. Férriz, A. Bernad, M. Mori, S. Fiorot, End-of-life of fuel cell and hydrogen products: a state of the art, Int. J. Hydrog. Energy 44 (25) (2019) 12872–12879, https://doi.org/10.1016/j.ijhydene.2018.09.176.
[14] A. Valente, D. Iribarren, J. Dufour, End of life of fuel cells and hydrogen products: from technologies to strategies, Int. J. Hydrog. Energy 44 (38) (2019) 20965–20977, https://doi.org/10.1016/j.ijhydene.2019.01.110.
[15] M. Kamiya, Y. Mori, T. Kojima, R. Sasai, H. Itoh, Recycling process for yttria-stabilized tetragonal zirconia ceramics using a hydrothermal treatment, J. Mater. Cycles Waste Manage 9 (1) (2007) 27–33, https://doi.org/10.1007/s10163-006-0168-3.
[16] A. Benedetto Mas, S. Fiore, S. Fiorilli, F. Smeacetto, M. Santarelli, I. Schiavi, Analysis of lanthanum and cobalt leaching aimed at effective recycling strategies of solid oxide cells, Sustainability 14 (6) (2022), https://doi.org/10.3390/su14063335.
[17] A. Al Assadi, D. Goes, S. Baazouzi, M. Staudacher, P. Malczyk, W. Kraus, et al., Challenges and prospects of automated disassembly of fuel cells for a circular economy, Resources Conserv. Recycl. Adv. (2023) 19, https://doi.org/10.1016/j.rcradv.2023.200172.
[18] S. Saffirio, S. Pylypko, S. Fiorot, I. Schiavi, S. Fiore, M. Santarelli, et al., Hydrothermally-assisted recovery of Yttria- stabilized zirconia (YSZ) from end-of-life solid oxide cells, Sustain. Mater. Technol. (2022) 33, https://doi.org/10.1016/j.susmat.2022.e00473.
[19] G.T. Yenesew, E. Quarez, A. Le Gal La Salle, C. Nicollet, O. Joubert, Recycling and characterization of end-of-life solid oxide fuel/electrolyzer ceramic material cell components, Resour. Conserv. Recycl. 190 (2023), https://doi.org/10.1016/j.resconrec.2022.106809.
[20] S. Sarner, N.H. Menzler, A. Hilgers, O. Guillon, Recycling and reuse strategies for ceramic components of solid oxide cells, ECS Trans. 111 (6) (2023) 1369–1378, https://doi.org/10.1149/11106.1369ecst.
[21] C. Kaiser, T. Buchwald, U.A. Peuker, Ultrasonic decoating as a new recycling path to separate oxygen side layers of solid oxide cells, Green Chem. 26 (2) (2024) 960–967, https://doi.org/10.1039/d3gc03189f.
[22] G.T. Yenesew, C. Nicollet, E. Quarez, Le Gal La Salle, A, Joubert O., Scalable recycling and characterization of end-of-life solid oxide cell ceramic component materials, Next Sustain. (2025) 6, https://doi.org/10.1016/j.nxsust.2025.100110.
[23] N. Minh, Solid oxide fuel cell technology - features and applications, Solid State Ionics 174 (1–4) (2004) 271–277, https://doi.org/10.1016/j.ssi.2004.07.042.
[24] W.Z. Zhu, S.C. Deevi, Development of interconnect materials for solid oxide fuel cells, Mater. Sci. Eng. A 348 (1–2) (2003) 227–243, https://doi.org/10.1016/s0921-5093(02)00736-0.
[25] K.J. Yoon, J.W. Stevenson, O.A. Marina, High performance ceramic interconnect material for solid oxide fuel cells (SOFCs): Ca- and transition metal-doped yttrium chromite, J. Power Sources 196 (20) (2011) 8531–8538, https://doi.org/10.1016/j.jpowsour.2011.06.089.
[26] J.C.W. Mah, A. Muchtar, M.R. Somalu, M.J. Ghazali, Metallic interconnects for solid oxide fuel cell: a review on protective coating and deposition techniques, Int. J. Hydrog. Energy 42 (14) (2017) 9219–9229, https://doi.org/10.1016/j.ijhydene.2016.03.195.
[27] M.A. Hassan, O.B. Mamat, M. Mehdi, Review: influence of alloy addition and spinel coatings on Cr-based metallic interconnects of solid oxide fuel cells, Int. J. Hydrog. Energy 45 (46) (2020) 25191–25209, https://doi.org/10.1016/j.ijhydene.2020.06.234.

[28] K.H. Jo, J.H. Kim, K.M. Kim, I.-S. Lee, S.-J. Kim, Development of a new cost effective Fe–Cr ferritic stainless steel for SOFC interconnect, Int. J. Hydrog. Energy 40 (30) (2015) 9523–9529, https://doi.org/10.1016/j.ijhydene.2015.05.125.

[29] A. Nechache, S. Hody, Alternative and innovative solid oxide electrolysis cell materials: a short review, Renew. Sust. Energ. Rev. (2021) 149, https://doi.org/10.1016/j.rser.2021.111322.

[30] F. Mohsenifar, A. Irannejad, H. Ebrahimifar, Development of Mn-Co and Mn-Co-CeO2 coatings on Crofer 22 APU steel for solid oxide fuel cell interconnects, J. Electrochem. Soc. 170 (12) (2023), https://doi.org/10.1149/1945-7111/ad0ff9.

[31] K.H. Tan, H.A. Rahman, H. Taib, Coating layer and influence of transition metal for ferritic stainless steel interconnector solid oxide fuel cell: a review, Int. J. Hydrog. Energy 44 (58) (2019) 30591–30605, https://doi.org/10.1016/j.ijhydene.2019.06.155.

[32] J. Mao, E. Wang, H. Wang, M. Ouyang, Y. Chen, H. Hu, et al., Progress in metal corrosion mechanism and protective coating technology for interconnect and metal support of solid oxide cells, Renew. Sust. Energ. Rev. (2023) 185, https://doi.org/10.1016/j.rser.2023.113597.

[33] M.J. Reddy, B. Kamecki, B. Talic, E. Zanchi, F. Smeacetto, J.S. Hardy, et al., Experimental review of the performances of protective coatings for interconnects in solid oxide fuel cells, J. Power Sources (2023) 568, https://doi.org/10.1016/j.jpowsour.2023.232831.

[34] S.E. Wolf, F.E. Winterhalder, V. Vibhu, L.G.J. de Haart, O. Guillon, R.-A. Eichel, et al., Solid oxide electrolysis cells – current material development and industrial application, J. Mater. Chem. A 11 (34) (2023) 17977–18028, https://doi.org/10.1039/d3ta02161k.

[35] T. Horita, Chromium poisoning for prolonged lifetime of electrodes in solid oxide fuel cells - review, Ceram. Int. 47 (6) (2021) 7293–7306, https://doi.org/10.1016/j.ceramint.2020.11.082.

[36] Y. Wang, W. Jiang, M. Song, Y. Zhang, S.-T. Tu, Effect of frame material on the creep of solid oxide fuel cell, Int. J. Hydrog. Energy 44 (36) (2019) 20323–20335, https://doi.org/10.1016/j.ijhydene.2019.05.220.

[37] K. Vishal, K. Mandeep, K. Gurbinder, S.K. Arya, P. Gary, Stacking designs and sealing principles for IT-solid oxide fuel cell, in: G. Kaur (Ed.), Intermediate Temperature Solid Oxide Fuel Cells, Matthew Deans, 2020, pp. 379–410, https://doi.org/10.1016/B978-0-12-817445-6.00011-9.

[38] K. Singh, T. Walia, Review on silicate and borosilicate-based glass sealants and their interaction with components of solid oxide fuel cell, Int. J. Energy Res. 45 (15) (2021) 20559–20582, https://doi.org/10.1002/er.7161.

[39] P.A. Lessing, A review of sealing technologies applicable to solid oxide electrolysis cells, J. Mater. Sci. 42 (10) (2007) 3465–3476, https://doi.org/10.1007/s10853-006-0409-9.

[40] X.-V. Nguyen, C.-T. Chang, G.-B. Jung, S.-H. Chan, W.-T. Lee, S.-W. Chang, et al., Study of sealants for SOFC, Int. J. Hydrog. Energy 41 (46) (2016) 21812–21819, https://doi.org/10.1016/j.ijhydene.2016.07.156.

[41] N. Mahato, A. Banerjee, A. Gupta, S. Omar, K. Balani, Progress in material selection for solid oxide fuel cell technology: a review, Prog. Mater. Sci. 72 (2015) 141–337, https://doi.org/10.1016/j.pmatsci.2015.01.001.

[42] M. Fallah Vostakola, Horri B. Amini, Progress in material development for low-temperature solid oxide fuel cells: a review, Energies 14 (5) (2021), https://doi.org/10.3390/en14051280.

[43] J. Mouginn, J. Laurencin, J. Vulliet, M. Petitjean, E. Grindler, S. Di Iorio, et al., Recent highlights on solid oxide cells, stacks and modules developments at CEA, ECS Trans. 111 (6) (2023) 1101–1113, https://doi.org/10.1149/11106.1101ecst.

[44] G. Cubizolles, S. Alamome, F. Bosio, B. Gonzalez, C. Tantolin, L. Champelovier, et al., Development of a versatile and reversible multi-stack solid oxide cell system towards operation strategies optimization, ECS Trans. 111 (6) (2023) 1677–1688, https://doi.org/10.1149/11106.1677ecst.

[45] A.S. Elcogen. https://elcogen.com/;.

[46] M. Noponen, J. Puranen, A. Alfano, H. Granö-Fabritius, Solid oxide stack development at elcogen, ECS Trans. 111 (6) (2023) 133–141, https://doi.org/10.1149/11106.0133ecst.

[47] Fiaxell Sarl. https://fiaxell.com/products/specialty-inks-powders-and-cells/cells; [accessed 25th of July.2024].

[48] L.G.J. De Haart, S.B. Beale, R. Deja, L. Dittrich, T. Duyster, Q. Fang, et al., Forschungszentrum Jülich – current activities in SOC development, ECS Trans. 103 (1) (2021) 299–305, https://doi.org/10.1149/10301.0299ecst.

[49] S. Gross-Barsnick, J. Malzbender, Q. Fang, Repair joining of glass-ceramic sealants for SOC stacks, ECS Trans. 103 (1) (2021) 1859–1865, https://doi.org/10.1149/10301.1859ecst.

[50] S. Harboe, A. Schreiber, N. Margaritis, L. Blum, O. Guillon, N.H. Menzler, Manufacturing cost model for planar 5 kWel SOFC stacks at Forschungszentrum Jülich, Int. J. Hydrog. Energy 45 (15) (2020) 8015–8030, https://doi.org/10.1016/j.ijhydene.2020.01.082.

[51] H. Ghezel-Ayagh, B.P. Borglum, Review of progress in solid oxide fuel cells at FuelCell energy, ECS Trans. 78 (1) (2017) 77–86, https://doi.org/10.1149/07801.0077ecst.

[52] FuelCell Energy Inc. https://www.fuelcellenergy.com/platform; [accessed 26th of November.2024].

[53] Fuelcellmaterials. https://fuelcellmaterials.com/; [accessed 25th of July.2024].

[54] Ningbo SOFCMAN Energy Technology Co., Ltd. https://sofc.com.cn/cpzx; [accessed 25th of July.2024].

[55] M. Pagliari, D. Montinaro, E. Martelli, S. Campanari, A. Donazzi, Experimental analysis of the effect of cathodic CO2 supply to industrial solid oxide fuel cells, ECS Trans. 111 (6) (2023) 673–680, https://doi.org/10.1149/11106.0673ecst.

[56] SolydEra SpA. https://www.solydera.com/en/business-areas-solutions/; [accessed 26th of November.2024].

[57] M. Lang, S. Raab, M.S. Lemcke, C. Bohn, M. Pysik, Long term behavior of solid oxide electrolyser (SOEC) stacks, ECS Trans. 91 (1) (2019) 2713–2725, https://doi.org/10.1149/09101.2713ecst.

[58] M. Preininger, B. Stoeckl, V. Subotić, F. Mittmann, C. Hochenauer, Performance of a ten-layer reversible solid oxide cell stack (rSOC) under transient operation for autonomous application, Appl. Energy (2019) 254, https://doi.org/10.1016/j.apenergy.2019.113695.

[59] A. Hauch, P.G. Blennow, K.N. Dalby, D.B. Drasbæk, T. Heiredal-Clausen, A. K. Padinjarethil, et al., The Topsoe perspective: from electrode nanostructures to MW scaled SOEC systems, ECS Trans. 111 (6) (2023) 1125–1133, https://doi.org/10.1149/11106.1125ecst.

[60] T.L. Skafte, J. Hjelm, P. Blennow, C. Graves, Reactivating the Ni-YSZ electrode in solid oxide cells and stacks by infiltration, J. Power Sources 378 (2018) 685–690, https://doi.org/10.1016/j.jpowsour.2018.01.021.

[61] L. Wang, M. Chen, R. Küngas, T.-E. Lin, S. Diethelm, F. Maréchal, et al., Power-to-fuels via solid-oxide electrolyzer: operating window and techno-economics, Renew. Sust. Energ. Rev. 110 (2019) 174–187, https://doi.org/10.1016/j.rser.2019.04.071.

[62] M. Shen, P. Zhang, Progress and challenges of cathode contact layer for solid oxide fuel cell, Int. J. Hydrog. Energy 45 (58) (2020) 33876–33894, https://doi.org/10.1016/j.ijhydene.2020.09.147.

[63] Z. Yang, G. Xia, P. Singh, J.W. Stevenson, Electrical contacts between cathodes and metallic interconnects in solid oxide fuel cells, J. Power Sources 155 (2) (2006) 246–252, https://doi.org/10.1016/j.jpowsour.2005.05.010.

[64] M.K. Rath, A. Kossenko, A. Kalashnikov, M. Zinigrad, Novel anode current collector for hydrocarbon fuel solid oxide fuel cells, Electrochim. Acta (2020) 331, https://doi.org/10.1016/j.electacta.2019.135271.

[65] J.H. Zhu, H. Ghezel-Ayagh, Cathode-side electrical contact and contact materials for solid oxide fuel cell stacking: a review, Int. J. Hydrog. Energy 42 (38) (2017) 24278–24300, https://doi.org/10.1016/j.ijhydene.2017.08.005.

[66] X. Montero, F. Tietz, D. Stöver, M. Cassir, I. Villarreal, Comparative study of perovskites as cathode contact materials between an La0.8Sr0.2FeO3 cathode and a Crofer22APU interconnect in solid oxide fuel cells, J. Power Sources 188 (1) (2009) 148–155, https://doi.org/10.1016/j.jpowsour.2008.11.083.

[67] D. Udomsilp, C. Lenser, O. Guillon, N.H. Menzler, Performance benchmark of planar solid oxide cells based on material development and designs, Energ. Technol. 9 (4) (2021), https://doi.org/10.1002/ente.202001062.

[68] N.H. Menzler, D. Schäfer, N. Kruse, R. Peters, F. Kunz, Solid Oxide Cells for Hydrogen Generation and Usage: From Materials to Systems 2023, CFI Ceramic Forum International / Ber. DKG 100 / 3, 2023, pp. 48–56.

[69] L. Blum, Q. Fang, S.M. Groß-Barsnick, L.G.J. de Haart, J. Malzbender, N. H. Menzler, et al., Long-term operation of solid oxide fuel cells and preliminary findings on accelerated testing, Int. J. Hydrog. Energy 45 (15) (2020) 8955–8964, https://doi.org/10.1016/j.ijhydene.2020.01.074.

[70] N.H. Menzler, D. Sebold, S. Zischke, SOC degradation: long-term and small-scale effects, ECS Trans. 91 (1) (2019) 719–729, https://doi.org/10.1149/09101.0719ecst.

[71] Y. Zheng, Q. Li, T. Chen, W. Wu, C. Xu, W.G. Wang, Comparison of performance and degradation of large-scale solid oxide electrolysis cells in stack with different composite air electrodes, Int. J. Hydrog. Energy 40 (6) (2015) 2460–2472, https://doi.org/10.1016/j.ijhydene.2014.12.101.

[72] J. Park, Y. Namgung, B. Singh, D. Shin, M.P.G. Hanantyo, S.-J. Song, Enhanced performance of reversible solid oxide fuel cells by densification of Gd0.1Ce0.9O2−δ (GDC) barrier layer/La0.6Sr0.4Co0.2Fe0.8O3−δ (LSCF6428)-GDC oxygen-electrode interface, J. Alloys Compd. (2024) 976, https://doi.org/10.1016/j.jallcom.2023.173296.

[73] M. Shiono, K. Kobayashi, T. Lannguyen, K. Hosoda, T. Kato, K. Ota, et al., Effect of CeO2 interlayer on ZrO2 electrolyte/La(Sr)CoO3 cathode for low-temperature SOFCs, Solid State Ionics 170 (1–2) (2004) 1–7, https://doi.org/10.1016/j.ssi.2004.02.018.

[74] I. Kim, S. Barnett, Y. Jiang, M. Pillai, N. McDonald, D. Gostovic, et al., Composite Cathode for High-Power Density Solid Oxide Fuel Cells. United States, 2004, https://doi.org/10.2172/882534. Medium: ED.

[75] Y.J. Xue, H. Miao, C.R. He, J.X. Wang, M. Liu, S.S. Sun, et al., Electrolyte supported solid oxide fuel cells with the super large size and thin ytterbia stabilized zirconia substrate, J. Power Sources 279 (2015) 610–619, https://doi.org/10.1016/j.jpowsour.2015.01.058.

[76] L. Mathur, Y. Namgung, H. Kim, S.-J. Song, Recent progress in electrolyte-supported solid oxide fuel cells: a review, J. Korean Ceram. Soc. 60 (4) (2023) 614–636, https://doi.org/10.1007/s43207-023-00296-3.

[77] Y. Liu, Z. Shao, T. Mori, S.P. Jiang, Development of nickel based cermet anode materials in solid oxide fuel cells – now and future. Materials reports, Energy 1 (1) (2021), https://doi.org/10.1016/j.matre.2020.11.002.

[78] A.K. Padinjarethil, F.R. Bianchi, B. Bosio, A. Hagen, Electrochemical characterization and modelling of anode and electrolyte supported solid oxide fuel cells, Front. Energy Res. (2021) 9, https://doi.org/10.3389/fenrg.2021.668964.

[79] D. Werner, U.A. Peuker, T. Mütze, Recycling chain for spent Lithium-ion batteries, Metals 10 (3) (2020), https://doi.org/10.3390/met10030316.

[80] M. Kaya, WPCB Recycling Chain and Treatment Options. Electronic Waste and Printed Circuit Board Recycling Technologies, 2019, pp. 59–68, https://doi.org/10.1007/978-3-030-26593-9_3.

[81] DIN 8580, DIN 8580:2003–09. Manufacturing Processes - Terms and Definitions, Division, 2003. DIN 8580:2003–09.

[82] DIN/TS 54405, DIN/TS 54405:2020–12, Construction Adhesives - Guideline for Separation and Recycling of Adhesives and Substrates from Bonded Joints, 2020.
[83] S. Sarner, N.H. Menzler, J. Malzbender, M. Hilger, D. Sebold, A. Weber, et al., Towards a scalable recycling process for ceramics in fuel-electrode-supported solid oxide cells, Green Chem. 27 (8) (2025) 2252–2262, https://doi.org/10.1039/d4gc05883f.
[84] S. Ahn, M. Rudolph, Development of fine particle mechanical separation processes with representative catalyst materials for recycling PEM water electrolyzers exploiting their wetting characteristics, ChemCatChem 16 (1) (2023), https://doi.org/10.1002/cctc.202300931.
[85] M. Mori, J. Gramc, D. Hojkar, A. Lotrič, F. Smeacetto, S. Fiorilli, et al., New life cycle inventories for end-of-life solid oxide cells based on novel recycling processes for critical solid oxide cell materials, Int. J. Hydrog. Energy 104 (2025) 635–650, https://doi.org/10.1016/j.ijhydene.2024.08.411.
[86] P. Semsari Parapari, M. Parian, J. Rosenkranz, Breakage process of mineral processing comminution machines – an approach to liberation, Adv. Powder Technol. 31 (9) (2020) 3669–3685, https://doi.org/10.1016/j.apt.2020.08.005.
[87] H. Schubert, Aufbereitung fester mineralischer Rohstoffe, 4th ed., Dt. Verl. für Grundstoffindustrie, Leipzig, 1989.
[88] C. Kaiser, U.A. Peuker, Recycling of raw materials in solid oxide cells: Ultrasonic decoating for mechanical liberation and separation of perovskite materials, in: XXXI IMPC-International Mineral Processing Congress, Society for Mining, Metallurgy & Exploration Inc. (SME), Washington D. C/National Harbor, MD, 2024, pp. 3276–3283.
[89] T. Leistner, M. Embrechts, T. Leißner, S. Chehreh Chelgani, I. Osbahr, R. Möckel, et al., A study of the reprocessing of fine and ultrafine cassiterite from gravity tailing residues by using various flotation techniques, Miner. Eng. 96-97 (2016) 94–98, https://doi.org/10.1016/j.mineng.2016.06.020.
[90] T. Leistner, U.A. Peuker, M. Rudolph, How gangue particle size can affect the recovery of ultrafine and fine particles during froth flotation, Miner. Eng. 109 (2017) 1–9, https://doi.org/10.1016/j.mineng.2017.02.005.
[91] A. Yáñez, N. Kupka, B. Tunç, J. Suhonen, A. Rinne, Fine and ultrafine flotation with the Concorde CellTM – A journey, Miner. Eng. (2024) 206, https://doi.org/10.1016/j.mineng.2023.108538.
[92] B.A. Wills, J.A. Finch, Wills' Mineral Processing Technology, 8th ed., Butterworth-Heinemann, Boston, 2016 https://doi.org/10.1016/c2010-0-65478-2.
[93] J. Erler, S. Machunsky, P. Grimm, H.-J. Schmid, U.A. Peuker, Liquid–liquid phase transfer of magnetite nanoparticles — evaluation of surfactants, Powder Technol. 247 (2013) 265–269, https://doi.org/10.1016/j.powtec.2012.09.047.
[94] A. Vanderbruggen, J. Sygusch, M. Rudolph, R. Serna-Guerrero, A contribution to understanding the flotation behavior of lithium metal oxides and spheroidized graphite for lithium-ion battery recycling, Colloids Surf. A Physicochem. Eng. Asp. (2021) 626, https://doi.org/10.1016/j.colsurfa.2021.127111.
[95] S. Ahn, S. Patil, M. Rudolph, Influence of surfactants on selective mechanical separation of fine active materials used in high temperature electrolyzers contributing to circular economy, Industr. Chem. Mater. (2024), https://doi.org/10.1039/d4im00044g.
[96] R.M.E. Silva, R. Poon, J. Milne, A. Syed, I. Zhitomirsky, New developments in liquid-liquid extraction, surface modification and agglomerate-free processing of inorganic particles, Adv. Colloid Interf. Sci. 261 (2018) 15–27, https://doi.org/10.1016/j.cis.2018.09.005.
[97] L.P. Wang, Y. Kanemitsu, G. Dodbiba, T. Fujita, Y. Oya, H. Yokoyama, Separation of ultrafine particles of alumina and zircon by liquid–liquid extraction using kerosene as the organic phase and sodium dodecylsulfate (SDS) as the surfactant collector for abrasive manufacturing waste recycling, Sep. Purif. Technol. 108 (2013) 133–138, https://doi.org/10.1016/j.seppur.2013.02.009.
[98] B. Fan, F. Li, Y. Cheng, Z. Wang, N. Zhang, Q. Wu, et al., Rare-earth separations enhanced by magnetic field, Sep. Purif. Technol. (2022) 301, https://doi.org/10.1016/j.seppur.2022.122025.
[99] L. Gao, Y. Chen, A study on the rare earth ore containing scandium by high gradient magnetic separation, J. Rare Earths 28 (4) (2010) 622–626, https://doi.org/10.1016/s1002-0721(09)60167-8.
[100] P. Boelens, Z. Lei, B. Drobot, M. Rudolph, Z. Li, M. Franzreb, et al., High-gradient magnetic separation of compact fluorescent lamp phosphors: elucidation of the removal dynamics in a rotary permanent magnet separator, Minerals 11 (10) (2021), https://doi.org/10.3390/min11101116.
[101] J. Oberteuffer, High gradient magnetic separation, IEEE Trans. Magn. 9 (3) (1973) 303–306, https://doi.org/10.1109/tmag.1973.1067673.
[102] R. Mahendiran, S.K. Tiwary, A.K. Raychaudhuri, T.V. Ramakrishnan, R. Mahesh, N. Rangavittal, et al., Structure, electron-transport properties, and giant magnetoresistance of hole-doped LaMnO3 systems, Phys. Rev. B Condens. Matter 53 (6) (1996) 3348–3358, https://doi.org/10.1103/physrevb.53.3348.
[103] A.O. Turky, M.M. Rashad, A.M. Hassan, E.M. Elnaggar, M. Bechelany, Optical, electrical and magnetic properties of lanthanum strontium manganite La(1-x)Sr (x)MnO(3) synthesized through the citrate combustion method, Phys. Chem. Chem. Phys. 19 (9) (2017) 6878–6886, https://doi.org/10.1039/c6cp07333f.
[104] D.J. Brett, A. Atkinson, N.P. Brandon, S.J. Skinner, Intermediate temperature solid oxide fuel cells, Chem. Soc. Rev. 37 (8) (2008) 1568–1578, https://doi.org/10.1039/b612060c.
[105] S. Hui, J. Roller, S. Yick, X. Zhang, C. Decès-Petit, Y. Xie, et al., A brief review of the ionic conductivity enhancement for selected oxide electrolytes, J. Power Sources 172 (2) (2007) 493–502, https://doi.org/10.1016/j.jpowsour.2007.07.071.
[106] Y. Liu, Effects of impurities on microstructure in Ni/YSZ–YSZ half-cells for SOFC, Solid State Ionics 161 (1–2) (2003) 1–10, https://doi.org/10.1016/s0167-2738(03)00271-6.
[107] Y. Zhang, X. Huang, Z. Lu, X. Ge, J. Xu, X. Xin, et al., Effect of starting powder on screen-printed YSZ films used as electrolyte in SOFCs, Solid State Ionics 177 (3–4) (2006) 281–287, https://doi.org/10.1016/j.ssi.2005.11.008.
[108] T. Kojima, Y. Mori, M. Kamiya, R. Sasai, H. Itoh, Disintegration process of yttria-stabilized zirconia ceramics using hydrothermal conditions, J. Mater. Sci. 42 (15) (2007) 6056–6061, https://doi.org/10.1007/s10853-006-1167-4.
[109] J.R. Wilson, S.A. Barnett, Solid oxide fuel cell Ni–YSZ anodes: effect of composition on microstructure and performance, Electrochem. Solid-State Lett. 11 (10) (2008), https://doi.org/10.1149/1.2960528.
[110] F. Thaler, D. Udomsilp, W. Schafbauer, C. Bischof, Y. Fukuyama, Y. Miura, et al., Redox stability of metal-supported fuel cells with nickel/gadolinium-doped ceria anode, J. Power Sources (2019) 434, https://doi.org/10.1016/j.jpowsour.2019.226751.
[111] L. Blum, P. Batfalsky, L.G.J. de Haart, J. Malzbender, N.H. Menzler, R. Peters, et al., Overview on the Jülich SOFC development status, ECS Trans. 57 (1) (2013) 23–33, https://doi.org/10.1149/05701.0023ecst.
[112] J. Lastam, D. Sergeev, D. Grüner, M. Müller, R. Schwaiger, Unlocking the value of end-of-life JÜLICH solid oxide cell stack interconnect assembly: a combined experimental and thermodynamic study on metallic resource recyclability, Metals 14 (4) (2024), https://doi.org/10.3390/met14040406.
[113] VDM Metals VDM®, Crofer 22 H. Werdohl, Germany, 2021.
[114] VDM Metals VDM®, Crofer 22 APU. Werdohl, Germany, 2022.
[115] Y. Wang, R. Pillai, E. Yazhenskikh, M. Frommherz, M. Müller, D. Naumenko, Role of temperature in Na2SO4–K2SO4 deposit induced type II hot corrosion of NiAl coating on a commercial Ni-based Superalloy, Adv. Eng. Mater. 22 (6) (2020), https://doi.org/10.1002/adem.201901244.
[116] X. Wang, J. Hedberg, H.-Y. Nie, M.C. Biesinger, I. Odnevall, Y.S. Hedberg, Location of cobalt impurities in the surface oxide of stainless steel 316L and metal release in synthetic biological fluids, Mater. Des. (2022) 215, https://doi.org/10.1016/j.matdes.2022.110524.
[117] J. Lastam, M. Müller, D. Sergeev, A. Specht, S.-O. Mongoljiibuu, R. Schwaiger, Transforming end-of-life SOC metallic components into commercial grade austenitic stainless steels, in: EFCF 2024. Lucerne, Switzerland, 2024.
[118] F. Kukurugya, P. Nielsen, L. Horckmans, Up-concentration of chromium in stainless steel slag and ferrochromium slags by magnetic and gravity separation, Minerals 10 (10) (2020), https://doi.org/10.3390/min10100906.
[119] European Commission, Study on the Critical Raw Materials for the EU 2023 - Final Report, 2023, https://doi.org/10.2873/12230.
[120] C. Rachmawati, J. Weiss, H.I. Lucas, E. Löwer, T. Leißner, D. Ebert, et al., Characterisation of the grain morphology of artificial minerals (EnAMs) in Lithium slags by correlating multi-dimensional 2D and 3D methods, Minerals 14 (2) (2024), https://doi.org/10.3390/min14020130.